POLITECNICO DI TORINO

Master's Degree in Automotive Engineering

Master's Thesis

Design and implementation of autonomous braking system for Formula Student Driverless application

Supervisor:

Prof. Andrea Tonoli

Candidate:

Samuel Ciocca

Co-supervisors:

Prof. Nicola Amati

Ing. Gennaro Sorrentino

Ing. Raffaele Manca

Ing. Eugenio Tramacere

Academic Year 2021/2022

Abstract

To achieve the autonomous drive, a vehicle must be able to do the perception of the environment, to elaborate the signals for the path planning and to perform the dynamic manoeuvres without any human intervention. For the perception part, the main sensors that are used are the radar, the lidar, the stereo camera and the ultrasonic sensors. For the path planning on the autonomous vehicles some dedicated hardware is present in order to elaborate the information coming from each sensor and to properly control the vehicle dynamics. For what concerns the dynamic manoeuvres, the development of systems that can properly reproduce human's inputs such as the steering action and the pedals pushing are necessary. An Autonomous Braking System will be the object of this thesis. Its function is useful both for autonomous vehicles and traditional ones since it is able to increase the safety when the human intervention cannot be performed. This kind of device can be implemented in different ways, such as through electric motors that directly move the pedal or with pumps that rise the oil pressure inside the braking lines. This device will be developed on the Formula Student prototype SC19D. The aim of this vehicle is to participate to Formula Student Driverless, a competition in which each team is composed by engineering students with the aim to design and build a fully autonomous vehicle. The Autonomous braking System developed in this thesis will be an adaptation of an already existing traditional brake pedal, equipped with two independent master cylinders and a balance bar, needed to make the partition of the brake effort between the front and the rear axle. The layout of the system will be composed by a servomotor that, through a pulley, actuates with a metal cable directly on the top of the brake pedal. After a short introduction in the first chapter, in which the context about the autonomous drive and the formula student competitions will be exposed, two models of the brake system will be developed. The first one will be a bidimensional model collapsed on the midplane, obtained by physical and geometrical considerations, that represent the brake pedal and the master cylinders. This model will be very simplified but useful to perform a rough sizing of the servomotor. Then, a parametric multibody 3d model will be carried out on MATLAB® Simulink. In this one the two master cylinders, the balance bar, the servomotor and the pulley with the metal cable will be modelled. From the results obtained by the simulations of the multibody model, some lookup tables will be realized to directly link the servomotor PWM control signal to the oil pressure inside the brake

lines. Moreover, a PID controller will be designed to realize a closed loop control on the oil pressure and to reduce the errors. The chapter 4 “Mechanical Implementation” will be dedicated to the design of the mechanical parts. In that section a more detailed design of the main mechanical components will be analysed. In the end, there will be an experimental campaign done directly on the vehicle. This will lead to important results to validate the architecture, the models and the control of the system.

Acknowledgements

I would like to thank Prof. Andrea Tonoli and Prof. Nicola Amati for supporting me in the drafting of the thesis, giving to me the possibility to work on a project to which I am very fond. I would thank my co-supervisors Gennaro Sorrentino, Raffaele Manca and Eugenio Tramacere for their help that has been fundamental.

My sincere thanks also go to every student on the team Squadra Corse Driverless, my hands will never forget all the braking oil they touched. In you I found a family where I learned and I had fun. Together we have grown a lot, reaching results that we thought unbelievable.

I would say thanks to my parents Luca and Monica that supported me in every choice, giving to me everything I needed even if it weren't possible. I would say thanks to my brother Joele that have been next to me all the time as a reference and as my best friend. I thank my grandparents Attilio and Marilena, my uncles Antonella e Franco and my grandfather Giovanni, who have been near to me in each little goal that brought me up to this day. You gave to me all your enthusiasm helping me get through difficult times. I would sincerely thank my friends and colleagues Alessandro and David. With you I learned the meaning of engineering and now we are all starting an exciting new life. I thank all my friends from Loano and from Genova, even if I were far from the sea, my heart has been always there. Finally, I would say thank to my fiancée Martina for every day and every evening spent studying together. You turned a duty into something special and without you this journey would be really hard.

Contents

Chapter 1 – Introduction

Autonomous drive

Cars are nowadays common as way of transport, and they let us to do things that even just in the previous century were unbelievable. The number of kilometres that we can cover in a day with our own car in a relative short time has a huge difference with respect to the begin of the last century. Moreover, to have an own car gives to people the psychological freedom to be able to go where they want when they want. The number of vehicles in the world has grown exponentially in a very short time. It's enough to think that there were 670 million vehicles in 1996, and just 342 million vehicles in 1976 [1], but looking at the collected data of 2022, 1.446 billion of cars have been registered in the world [2]. This exponential trend brought the OEMs to find new ways to improve the vehicles, both on reducing pollutant emissions, efficiency, safety, but also on increasing customer satisfaction. One of the new trends that covers each of these aspects are the ADAS (Advanced Driver Assistance Systems) and more in general the Autonomous drive. The document "J3016_202104" [3] provides six levels of automation related to the action that a vehicle can perform. These levels are collected in the figure below.

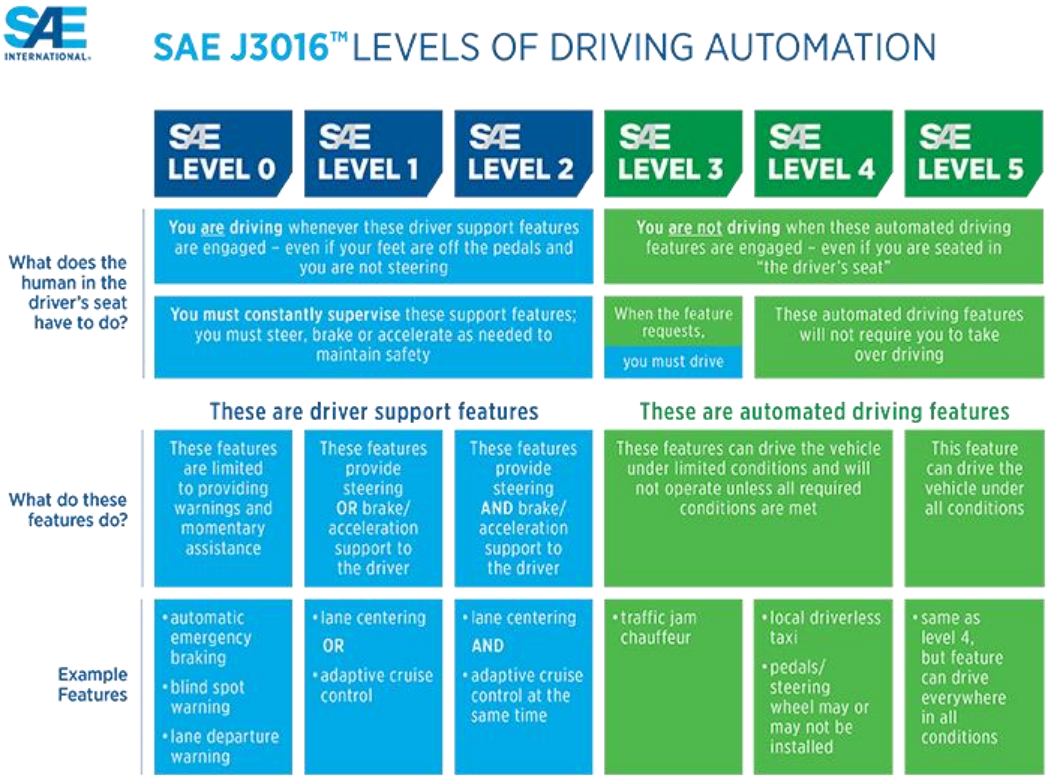

Figure 1 SAE J3016TM levels of Driving Automation

As shown in Figure 1, the features of each level are really differentiated and, while the level increases, also the complexity of the corresponding autonomous features increases. The realization of higher levels is so difficult from the engineering point of view, that today vehicles that are totally autonomous are not still commercialized and the prototypes that exist are not ready for the market yet. Lower levels have not a big impact for the driver and are supposed to be only a support during manual driving. Higher levels instead are more invasive introducing also features that don't require any human intervention to perform complex manoeuvres. The autonomous drive can bring a lot of advantages in terms of safety (i.e., warnings, automating braking) and in terms of emissions reduction (i.e., traffic jam chauffer, adaptive cruise control). Ideally a machine can achieve reaction time lower compared to any human and so it can help the driver in dangerous situations. For instance, if the vehicle risks impacting against an obstacle, a well-designed autonomous assistance could identify it by means of the sensors and the vehicle's control could react in time to avoid a fatal accident. The same thing is true for what concerns the circumstances in which the driver can't intervene to control the vehicle. If for instance the driver has a stroke, an autonomous vehicle could be able to self-drive up to a safe place and call an ambulance. For what concerns the reduction of pollutant emissions the autonomous drive could introduce new opportunities like the possibility to realize fleet of vehicle that drive at constant speed in highways or connected vehicle that reduce the amount of traffic in city centre. The introduction of autonomous drive has also a big impact on business, marketing, and customer satisfaction. In the era of digitalization in which the customer is always interested in new technologic features, the autonomous drive increases the value of the product. Autonomous drive gives the opportunity to explore a new way of think not only private vehicles but also the public infrastructure. An interesting example are the autonomous public transportation vehicles (APTVs). These vehicles are supposed to replace traditional public transport (PT) that are driven by human intervention. The level of complexity of a fully autonomous vehicle is high and as seen from "J3016_202104" document, to achieve a complete autonomous drive the vehicle must be able to perform a lot of actions without human intervention. Anyway, if a controlled environment like a city centre is considered, the autonomous drive could be already very efficient today. The evaluation factors of an autonomous public transportation vehicle can be highlighted as follow [4]:

- Performance expectancy: the autonomous shuttles have more advantages compared to the traditional ones. Anyway, people sometimes still don't trust this new technology and prefer to make the journey on feet in normal circumstances.
- Effort expectancy: Lower is the effort to use an autonomous shuttle, better is the attitude towards this means of transports. So, associate this service with a low complexity human to machine interface is important in order to motivate people towards their use.
- Safety: factor related to safety issues concerns traffic, limitations due to absence of a driver, fear of incivilities and of invasion of data privacy. These factors about automation negatively influence the attitude toward autonomous mobility. The absence of a driver impacts negatively on customers experience since there is no human assistance, that is necessary for instance in case of asking information or assistance to people with disabilities. For what concerns data privacy if a vehicle is autonomous and connected, it could be subject to hacking risk, so informatic security is a key factor in order to make these vehicles safe from the customer point of view.
- Service characteristics: autonomous shuttles in this moment are more efficient compared to traditional ones since their frequency can be higher with less retards. Anyway, their speed is lower. Accordingly, it seems that people prefer to use autonomous vehicle for short journeys, but if a long trip is required, they usually choose the traditional ones.
- Vehicle characteristics: even if autonomous shuttles travel at low speeds, if their internal algorithm is not properly designed, they could perform abrupt breaking or steering manoeuvres that negatively impact on customer's comfort.
- Symbolic-affective system evaluation

Autonomous drive in the motorsport field

The autonomous drive has a lot of interest also for the competition world. In driverless competitions the vehicles are no more driven by human's intervention, but all the decisions are taken by an internal algorithm and the outputs are given by electromechanical actuators. The challenge is to design a vehicle able to go faster on the track but also with a more robust control compared to the opponents. The autonomous race prototypes are interesting because an autonomous vehicle theoretically could drive also faster than a human, so a lot of new paths could be developed in terms of high-

performance vehicles in the future. Recently, this field grown a lot and new competitions born. An example is the Indy Autonomous Challenge [5] that is the first head-to-head autonomous race car competition. In this challenge the aim is to race in traditional tracks in a head-to-head passing competition. The design behind an extreme manoeuvre such as the overtake at high speed in which each vehicle is close to each other is a big challenge for an autonomous vehicle application. The research in the competition field is important both for race purposes but also for real-world scenarios. The improvements that can be done on the race prototypes can also be applied on passenger vehicles in order to improve the performances and the safety in dangerous highway conditions. Moreover, the overtake manoeuvres are also critical from human perception point of view both in the cases in which people are inside of the overtaking or the overtaken vehicle. The human perception of this manoeuvres can be synthetized in "(i) pull-in distance after the overtake, (ii) occupant perspective: driving a vehicle that is being overtaken or being in an autonomous vehicle that is overtaking another vehicle, and (iii) the effect of traffic context; whether ratings of an overtaking manoeuvre are influenced if the overtaking vehicle is being followed by a third vehicle" [6]. The scenario in which this manoeuvre can be performed is different in the case in which other vehicles are also autonomous or are driven by humans. Pushing vehicle's performances to the limit, the contribution of the motorsport research can help in terms of research in passenger cars.

Formula student driverless

Formula Student Driverless (FSD) is a competition between engineering students in which the aim is to build a fully autonomous high-performance vehicle. It is a subcategory of the Formula Student Championship, that first held by the Society of Automotive Engineers in 1979 [7]. The prototypes competing in this competition must be designed according to the rules imposed by the championship organization. Each team is composed by student from different universities and each of them can bring its contributes and idea to build their prototype. This means that each team can reach the same target building systems that are totally different from each other, bringing a lot of new ideas that could be used in the future not only on the track but also in other engineering fields. For instance, vehicles can be equipped different type of powertrains. The propulsion can be done both with an internal combustion engine or with electric motors. Therefore, also the gearbox can be totally different since in the first case usually it is usually derived from motorbike field, while in the second case there is only a fixed gear. For the chassis each

team can choose to realize a full carbon monocoque or a tubular frame. In each design feature all the choices must be motivated with calculations and models and the results must be compliant with the rulebook. The main organizations are FSG (Formula Student Germany) and FSAE, each of one has a different rulebook.

The competition is divided into static and dynamic events. The static events are the ones in which basically the car must not perform any dynamic actions. The points are gained due to the engineering choices during presentations that students must do in front of some judges. In this first part the judges evaluate the design of the prototype and a business plan about the project presented by each team. The dynamic events are the ones in which the vehicle must go on the track performing three different stages: acceleration, trackpad and endurance. In the driverless category the track is composed by cones with different colours:

- Blue cones: represent the left limit of the track
- Yellow cones: represent the right limit of the track
- Orange cones: represent the end of the track

The aim of the vehicle is to detect these cones with the sensors to map them position and find the optimal trajectory to complete a lap.

The driverless vehicles in this competition must always maintain the possibility to be driven manually [8], so the actuators must be packaged inside the chassis in the way that the human movement are not constricted during manual driving.

As a member of the Formula Student Team Squadra Corse PoliTo Driverless, the vehicle that will be treated in this thesis will be SC19D. This prototype has been previously built in 2019 by the team Squadra Corse PoliTo in order to participate to the Driver Competition and it has been converted by our team in a driverless prototype for the Season 2022.

Figure 2 SC19D, team Squadra Corse Polito Driverless, Varano de Melegari 2022

Perception and Path Planning on SC19D

As an autonomous vehicle, SC19D is equipped with different sensors with the aim to detect the environment. In particular in the front part there is a Velodyne VLP16 LiDAR, that is needed to recreate the environment in three dimensions thanks to the action of laser rotating signals [9]. On the top of the main hoop there is a ZED stereo camera that can detect the objects on the front of the vehicle and detect their depth thanks to trigonometric considerations [10]. In Formula Student Driverless the stereo camera is essential because it allow to collect information about the colour of each cone to understand the limit of the track. From the information obtained by these two main sensors the internal logic can elaborate the sensor fusion to have a good estimation of the position of each cone on the track with respect the relative position of the car.

Figure 2 Velodyne VLP16 LiDAR

Figure 3 ZED stereo camera

The data collected by these sensors are then processed by an NVIDIA Jetson AGX-Xavier to calculate the optimal path planning of the vehicle. In this last there, is also a managing of the acceleration of the vehicle along each direction and so the dynamic manoeuvres must be correctly controlled by means of dedicated electromechanical actuators.

Electromechanical actuators

In order to perform the dynamic manoeuvres, the vehicle must be equipped with dedicated electromechanical actuators. The e-powertrain of the vehicle considered in this thesis is composed by four in-wheel internal permanent magnet motors. Each of them has a fixed

epicycloid reducer that links its motion to the respective wheel. To achieve a full autonomous drive, the actions that must be performed are principally the control of the longitudinal and the lateral dynamic. To do this is necessary to actuate on the accelerator pedal, on the brake pedal and on steering wheel without any human intervention. The accelerator pedal control is the simplest one: since the vehicle is driven by wire, the throttle command is based on two potentiometer that send to the ECU two redundant signals for safety reasons: if there is a fault on one of these, the other one can still work [11]. Moreover also plausibility consideration can be done on the two received signals in order to understand if there is any problem. A physical actuator is not necessary to perform this action since those potentiometers can be bypassed directly sending the control unit the desired electric signal proportional to the target pedal position. The situation is different for what concerns braking and steering manoeuvres where, since are performed by the force applied by the driver's feet on the pedal and by the torque produced by arms on the steering wheel, the design of dedicated electromechanical actuators is needed.

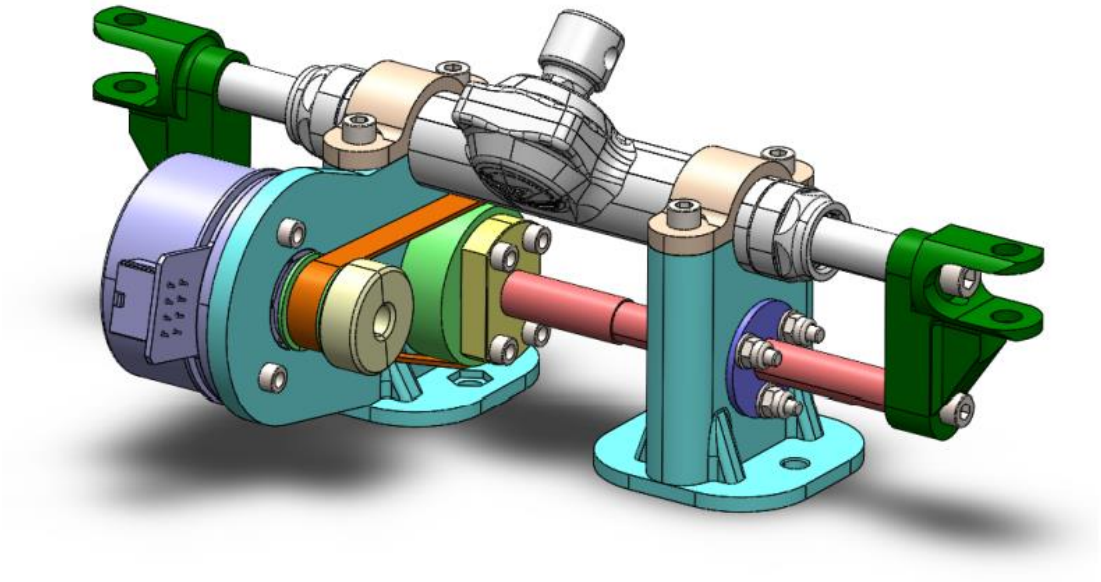

Figure 4 Steering actuator of SC19D

The steering system actuator realized for the SC19D is composed by an endless screw actuated by a DC brushless motor supported by an Aluminium Frame [12]. It supposed to replace the torque applied on the steering column acting directly on the clevis that move the steering mechanism. Thanks to its design this device doesn't interfere with driver movement so it is compliant to the championship rulebook [7].

According to the championship rules [7], the autonomous brake for a FSD vehicle must be divided into two different devices: an Emergency Braking System (EBS) and an Autonomous System Brake (ASB). The aim of the EBS is to actuate the brakes in emergency manoeuvres and for safety reasons it must be a passive system. As a passive system it must be able to actuate the brakes even if the electric power is not available, for this reason its power source cannot be electric. The EBS equipped on SC19D is powered by pressurized air contained in high pressure canisters. As shown in Figure 5, the air pressure is regulized by means of differential solenoid valves. These valves take closed the passage of the air until they receive an electric signal. Since the system is passive, solenoid valves are of the type "normally open", so they are always open during their de-energized condition. The air to oil interface is done by the pressure intensifiers designed to guarantee optimal performances in terms of response and pressure [13].

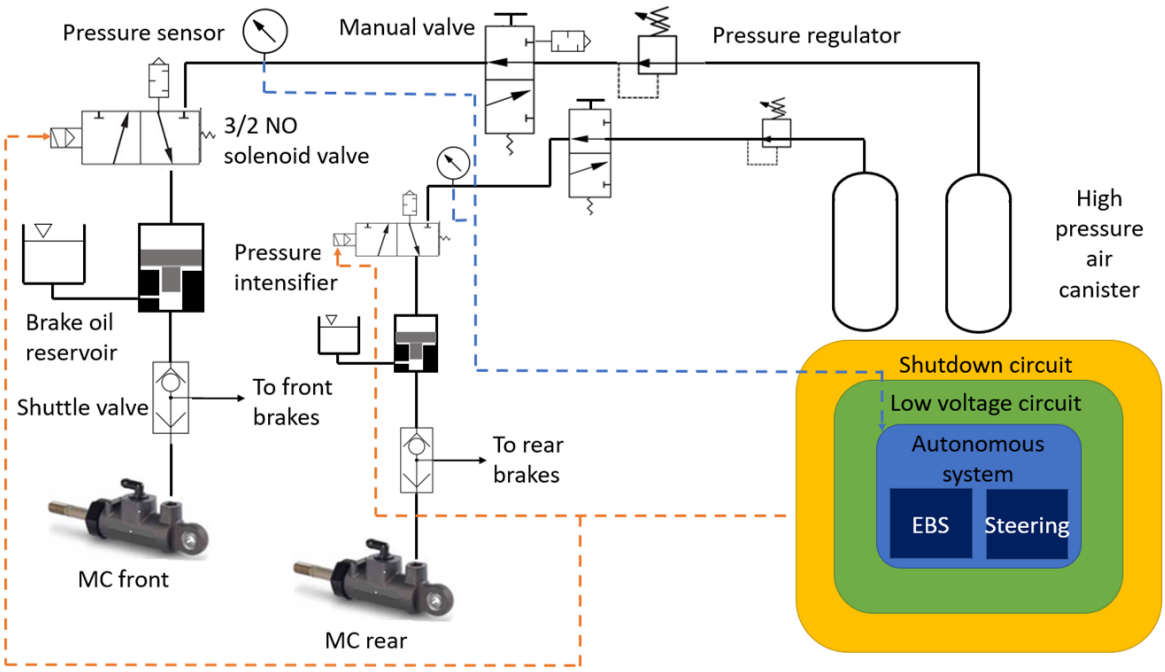

Figure 5 EBS layout

Autonomous System Brake

An autonomous system brake is a device with the aim to autonomously brake the vehicle with a proper deceleration and in safety condition. Since it supposes to replace the human mechanical input on the bake pedal, it must be able to do multiple actuations during a driving cycle. To be compliant with the regulation it must satisfy some design constraints.

The most important ones from which we'll start to develop the system and size each component are:

- it must be able to guarantee at least 4 $^{m}/_{s^2}$ of deceleration under dry track conditions [7]
- it must not interfere with manual driving [7].

The system will be equipped on an already existing prototype with its own manual brake system. The ASB developed in this thesis will be integrated in the manual braking system. The layout of the manual braking pedal is the following:

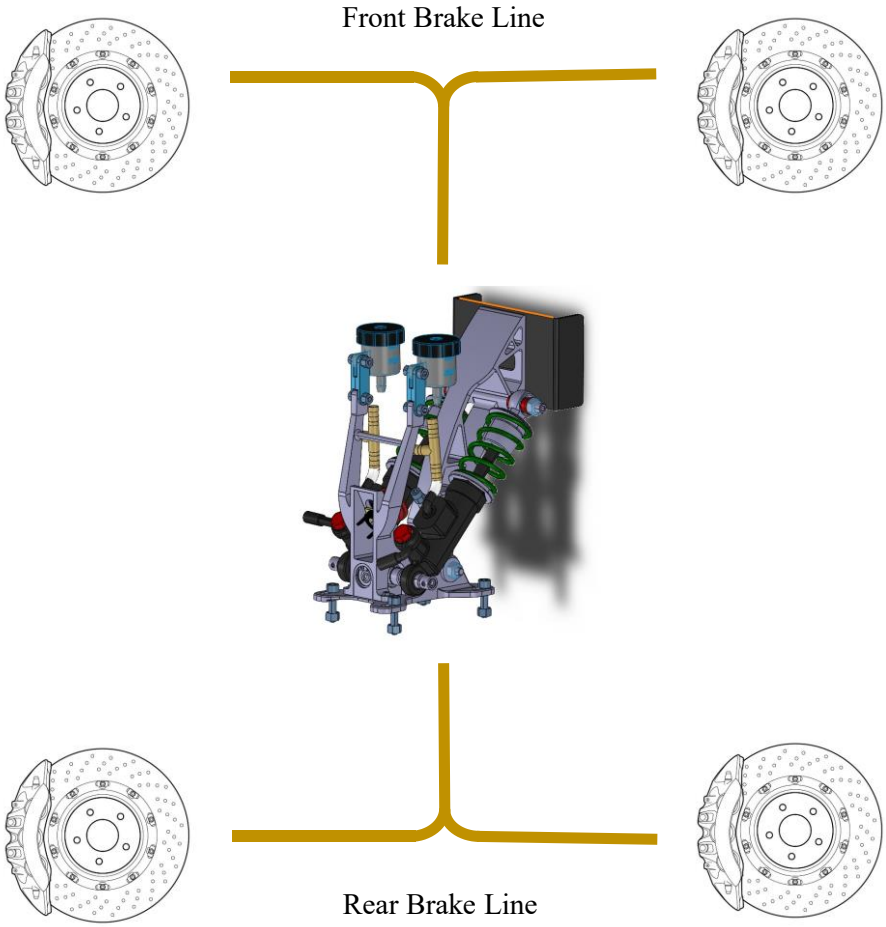

Figure 6 Manual Brake Line

The brake line equipped on the SC19D is of the type "front rear split", that means that the input on the brake pedal generates a rise of pressure on two different brake lines: one dedicated to the front axle and one dedicated to the rear axle. In common passenger cars application, the split of the two lines is of the type of "diagonal split" [14]. This solution

that is shown in the picture below is characterized by a brake line for the front right and rear left brake caliper and one for the front left and rear right one.

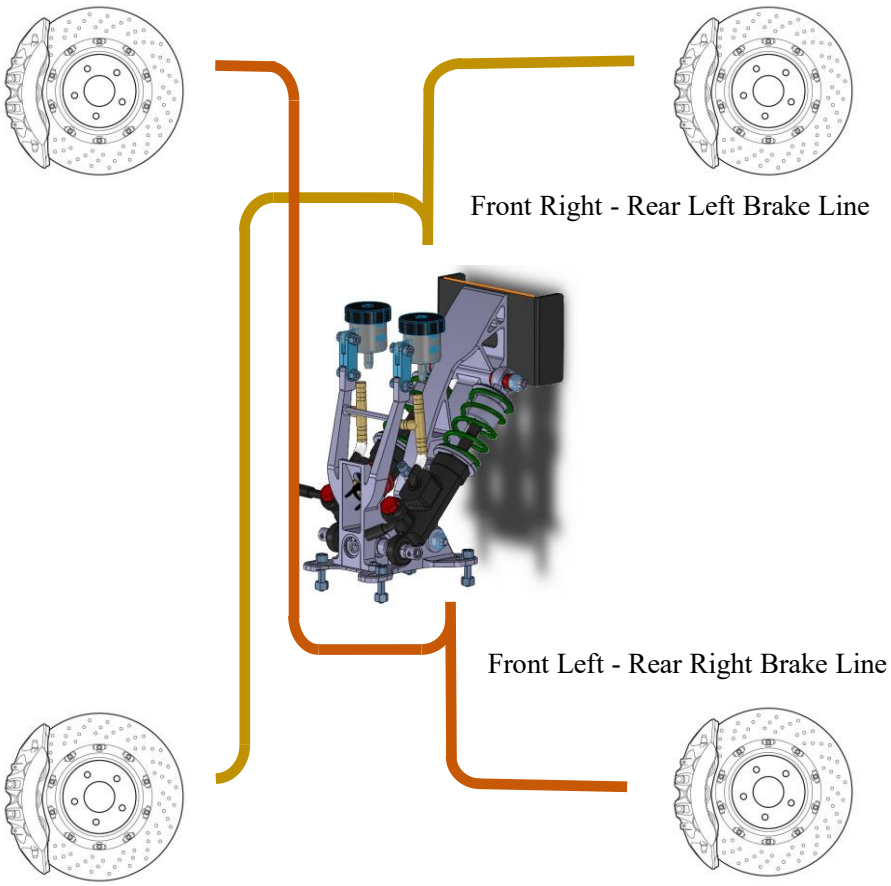

Figure 7 Diagonal Split Brake Line

On a vehicle the diagonal split brake line is adopted in order to increase the passenger safety. If due to the high pressure there is a leak of oil and a drop of brake effort on one of the two lines, the vehicle still has one braking wheel on the front and one braking wheel on the rear axle, independently from which line is broken. Considering instead a front rear split line if there is a fault, it will totally deactivate the braking effort on one of the two axles.

Considering the simplified three degrees of freedom model the following equations that describe the handling can be obtained [15]:

$$x_N = \frac{a * C_f - b * C_r}{C_f + C_r}$$

Where:

- x_N is the neutral steering point.

- a is the distance between the front axle and the centre of gravity of the vehicle.
- b is the distance between the rear axle and the centre of gravity of the vehicle.
- C_f is the cornering stiffness of the front axle.
- C_r is the cornering stiffness of the rear axle.

If x_N is null, the vehicle is neutral steering. If x_N is greater than zero, the vehicle behaviour will be oversteering while if it is lower than zero the vehicle will be more understeering.

Considering the cornering stiffness coefficients, the interaction between the longitudinal and the cornering force on the tire contact patch can be modelled with the so-called elliptical model:

$$C = C_0 \sqrt{1 - \left({F_x}/{\mu_x F_z}\right)^2}$$

Where:

- C is the cornering stiffness.
- C_0 is the maximum cornering stiffness corresponding to a condition with longitudinal force F_x null.
- F_x is the longitudinal force on the tire contact patch.
- μ_x is the longitudinal friction coefficient between the tire and the ground.
- F_z is the vertical force on the tire contact patch.

Combining the equation regarding the neutral steering point and the one of the lateral stiffness is possible to correlate the understeering/oversteering behaviour in function of the variation of the cornering stiffness. Going back to the fault on the two brake line layouts is possible now to understand why the diagonal split is safer. If one braking wheel on the front axle and one braking wheel on the rear axle are lost, in first approximation the handling behaviour of the vehicle remains unchanged. If instead the vehicle has a front-rear split layout, two possible scenarios can happen:

- A fault on the front axle would lead to an increment on the lateral stiffness of this last because there will be no longitudinal force on it anymore. Therefore, the neutral point will be shifted toward increasing the oversteering behaviour with the risk of spun. This is a dangerous scenario.

- A fault on the rear axle would lead to an increment of the lateral stiffness of this last because there will be no longitudinal force on it anymore. Therefore, the neutral point will be shifted backward increasing the understeering behaviour. This is a safer scenario.

So the diagonal split is safer since in case of fault the vehicle will be still safe independently from which brake line is broken.

In high performance vehicles, usually the front-rear split is adopted in order to have a different braking effort on the front and rear axle. In order to regulate this split, a the balance bar on the brake pedal is usually adopted.

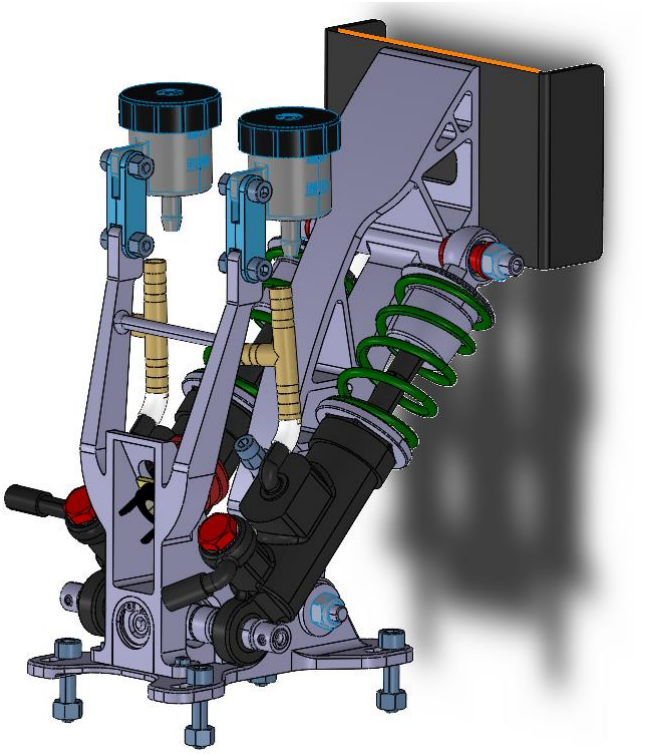

Figure 8 brake pedal assembly with two master cylinders and a balance bar

The brake system of SC19D shown in Figure 8 is characterized by the use of two different master cylinders (one of the front axle and one for the rear axle) and a balance bar.

The balance is an adjustable lever with the aim to regulate the partition of the brake effort between the front and the rear line [16]. When the balance bar is centered, it pushes equally on both the master cylinders. When it is moved towards a master cylinder, it will press more the other one. The reason of this behaviour is due to the following static equilibrium.

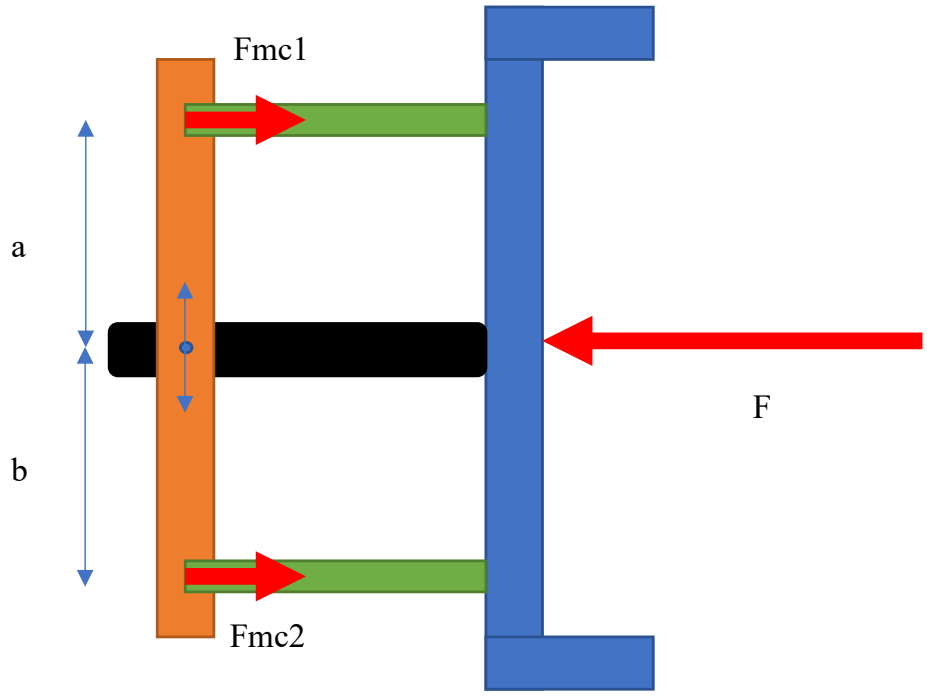

Figure 9 schematization of the brake pedal seen from above

$$Fmc1 + Fmc2 = F$$

$$Fmc1 * a = Fmc2 * b$$

Where:

- Fmc1 is the force actuated on the master cylinder 1.
- Fmc2 is the force actuated on the master cylinder 2.

Due to the body equilibrium showed in the formulas above, the relation between effort distribution and balance bar position is proved. If $a > b$, then $Fmc2 > Fmc1$ and so the effort on the brake line relative to master cylinder 2 is higher respect to the one on master cylinder 1. Same thing is true vice versa.

The layout of the brake line is composed by 4 disc brakes with 4 cylinders fixed calipers on the front line and 2 cylinders fixed calipers on the rear line. To estimate the needed the pressure inside the brake lines necessary to achieve at least 4 $^{m}/_{s^2}$ of deceleration, a longitudinal simplified model of the vehicle has been done [17]. The vehicle has been modelled without compliances and neglecting the slip of the tires. The only degree of freedom of this model is the longitudinal motion [18].

$$F_{x1} = \mu_x * F_{z1} = \mu_x * mg * (b - \left(\frac{h}{g}\right) * \ddot{x})/l$$

$$F_{x2} = \mu_x * F_{z2} = \mu_x * mg * (a + \left(\frac{h}{g}\right) * \ddot{x})/l$$

$$m * \ddot{x} = F_{x1} + F_{x2}$$

Where:

- Fx1 is the longitudinal force on the front tire ground contacts.
- Fx2 is the longitudinal force on the rear tire ground contacts.
- μ_x is the friction coefficient between ground and tire.
- m is the vehicle mass.
- g is gravitational acceleration.
- a is the distance between the front axle and the centre of gravity of the vehicle.
- b is the distance between the rear axle and the centre of gravity of the vehicle.
- h is the height of the centre of gravity of the vehicle with respect to the ground.
- $\ddot{x}$ is the vehicle longitudinal acceleration.

In order to consider the braking torque developed by the brake disks the following equation as been considered:

$$T = \frac{\mu_k P \pi D_b^2 R_m N}{4}$$

Where:

- T is the brake torque.
- P is the applied brake pressure.
- N is the number of brake pads in disc brake assembly.
- μ_k is the disc pad-rotor coefficient of kinetic friction.
- D_b is the brake actuator bore diameter.
- R_m is the mean radius of brake pad force application on brake rotor.

Furthermore, if we consider a balance bar position that makes the partition between the front and the rear line neutral, and we reduce all the torque contributions to a singular equivalent wheel, the brake torque T can be seen as:

$$T = F_x * R_e = m * \ddot{x} * R_e$$

Where R_e is the tire effective radius.

Due to the regulations, the vehicle must achieve during autonomous brake at least a longitudinal target of deceleration equal to 4 $^{m}/_{s^2}$. Using the previous equations, the acceleration target can be converted in a request of pressure at the braking lines. Since the brake calipers on the front axle have 4 pistons and the ones on the rear axle have 2 pistons, the total number of pistons N is:

$$N = N_{front\ left} + N_{front\ right} + N_{rear\ left} + N_{rear\ right} = 12$$

Data:

m	180 Kg
$\ddot{x}$	4 $^{m}/_{s^2}$
R_e	0.237 m
μ_k	0.4
D_b	0.024 m
R_m	0.15 m
N	12

Table 1 values of the parameter needed to the minimum pressure calculation

$$P = \frac{4m\ddot{x}R_e}{\mu_k \pi D_b^2 R_m N} = 5.24\ bar$$

So, the minimum brake oil pressure that this system must develop in order to be compliant with the formula student rulebook is 5.24 bar. This pressure is not enough to perform strong deceleration such as an emergency brake. So, to decide a higher peak pressure as dimensioning target allows is convenient to reach good performances during dynamic manoeuvres. During the tests on the emergency braking system (EBS) has been noticed that a value around 25 bar were enough to reach satisfying brake distances even at high speeds. Moreover, if a pressure of 25 bar is considered, it leads to a safety factor almost equal to 5 with respect the initial target of 5.24 bar. Therefore, the following target for the ASB development has been chosen:

$$P_{target} = 25bar.$$

Possible solutions for ASB development and the State of Art of autonomous braking:

The solutions that can be adopted for an autonomous system brake are different, here are reported some possible layouts that have been considered.

Electric oil pump:

A possible way to develop an ASB system could be the one to use the same principle of a Brake by Wire system (BBW). In Brake by Wire the oil pressure inside the brake lines is not actuated directly by the motion of the pedal but there is an electric pump that generates the needed pressure to slow down or stop the vehicle. In this system pedal and brake are mechanically decoupled and the pedal is needed only to move a travel sensor [19]. This kind of system are today really promising even in terms of safety [20], so the design of this solution could be supported by the state of art of brake by wire system reached today.

The introduction of an oil pump as in BBW after the pedal with the introduction of a or valve could be schematized as follows:

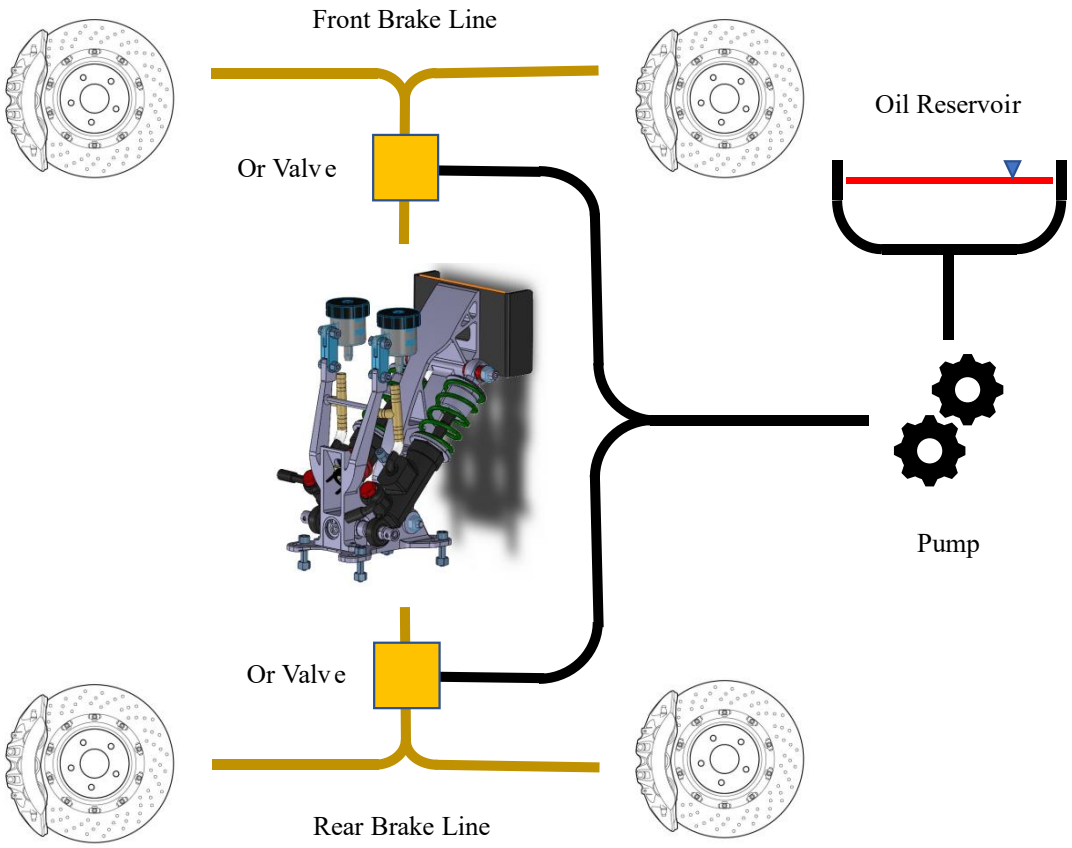

Figure 10 electric oil pump layout

Looking at this solution some pro and cons can be highlighted.

PRO:

- easy integration inside the already existing vehicle: an oil pump can be added to the braking line introducing an additional line without changing almost anything else inside the prototype. The position of the pump can be decoupled by the position of the pedal, and it allows a lot of freedom in terms of packaging inside the monocoque.
- easy control of the system: the behaviour of an electric pump is easy to control and manage.

CONS:

- High cost: the price of a pump that can develop at least 25 bar is high. The cost is further increased if the pump has also small size in terms of volume and weight to be fitted inside the monocoque.

Linear actuator

A linear actuator is an electromechanical actuator that generates straight motion [21]. Usually, it converts rotational motion into push or pull straight movement. The idea of this solution is to use a linear actuator to move a piston that enters inside the braking line. During its action it pushes the oil to increase the pressure or pull the piston to reduce it. The principle is really similar to the one of the electric pump solution and also the pro and cons are almost the same.

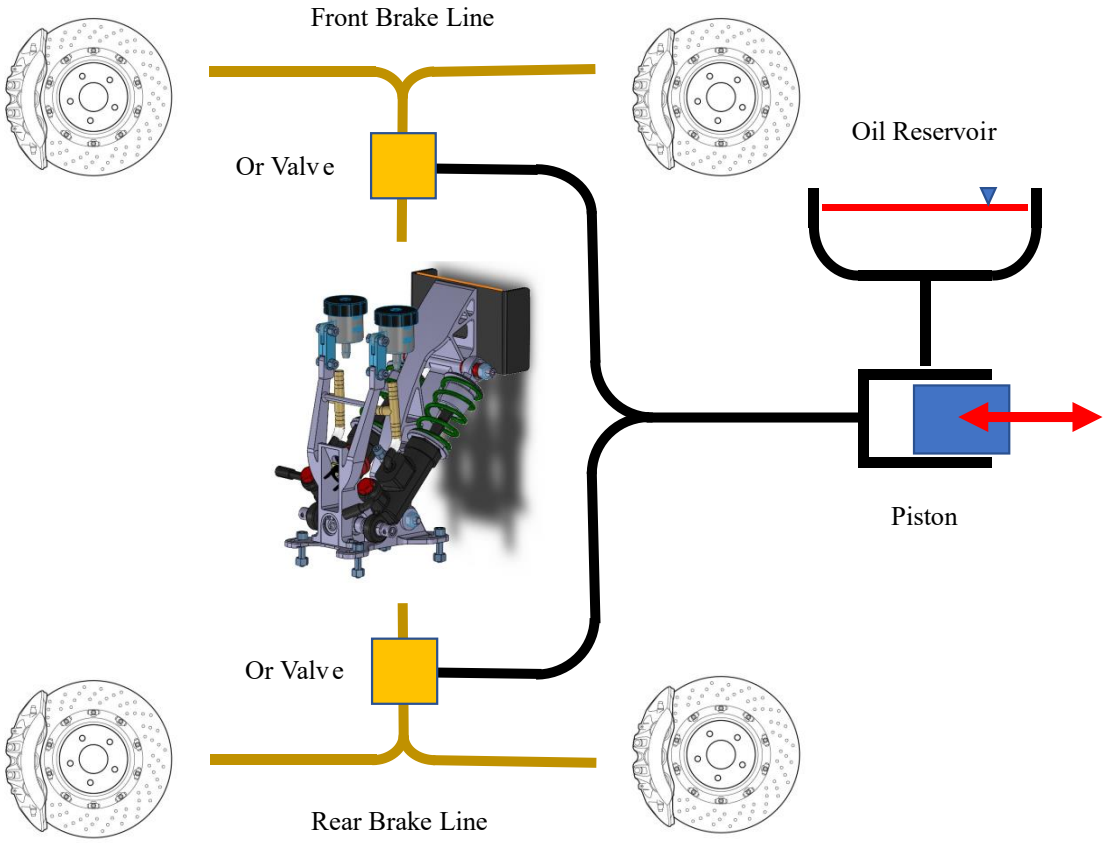

Figure 11 Linear actuator Layout

PRO:

- easy integration inside the already existing vehicle: a linear actuator can be added in each point of the braking line introducing without changing almost anything else inside the prototype. The position of the linear actuator can be decoupled by the position of the pedals and other elements, and it allows a lot of freedom in terms of packaging inside the monocoque.
- easy control of the system: the behaviour of a linear actuator is easy to control and manage.

CONS:

- High cost: the price of a linear actuator that can develop at least 25 bar is high.

Pressurized air

The use of pressurized line on board is already commonly diffused on commercial vehicles where it is used to provides comfort (air suspension) and safety (air brake system) [22]. The idea of this design is to use as energy source the pressurized air. The biggest advantage is the one to share the same intensifier of the EBS system to generate

pressure inside the braking oil starting from pressurized air. During a driving cycle the number of actuations cannot be limited by the air storage capability inside the canisters. A limited number of braking actuations would mean that after a certain number of brake event the vehicle could not decelerate anymore even in case of emergency. Due to that reason an additional electromechanical air compressor is needed to keep almost constant the pressure inside the canisters and to recharge them it when it is necessary.

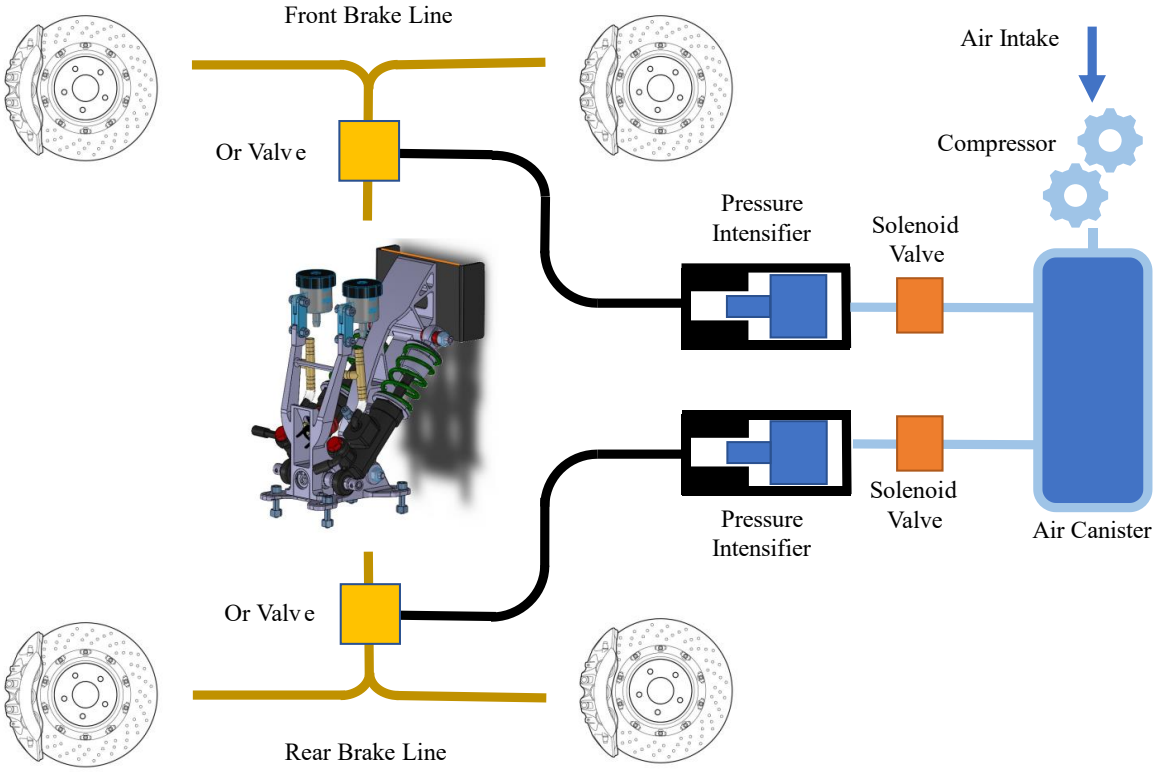

Figure 12 Pressurized Air Layout

Some advantages and reasons for the choice of this kind of system are:

- Easy integration inside the monocoque: compressed air can be stored inside little canisters and so packaging is not difficult. Same thing for the air compressor.
- Low complexity in control: the electromechanical pneumatic valves [23] and the compressor control is easy.
- The same hardware of already existing EBS can be adopted and so cost is not increased by the realization of new pressure intensifiers.

CONS:

- High cost: high frequency electromechanical pneumatic valves are expensive.

- High complexity of the layout: differently from previous design, in this case the integration is more difficult and a whole new air pressure line must be realized.

Actuate directly on the pedal

The idea is to build an actuator able to directly actuate force on the brake pedal emulating the same action that a human foot should do. As power source a high torque servomotor has been chosen. The mechanical interface between the servomotor and the top of the pedal is done by means of a metal cable. This cable will be coiled by a pulley motorized by the servomotor.

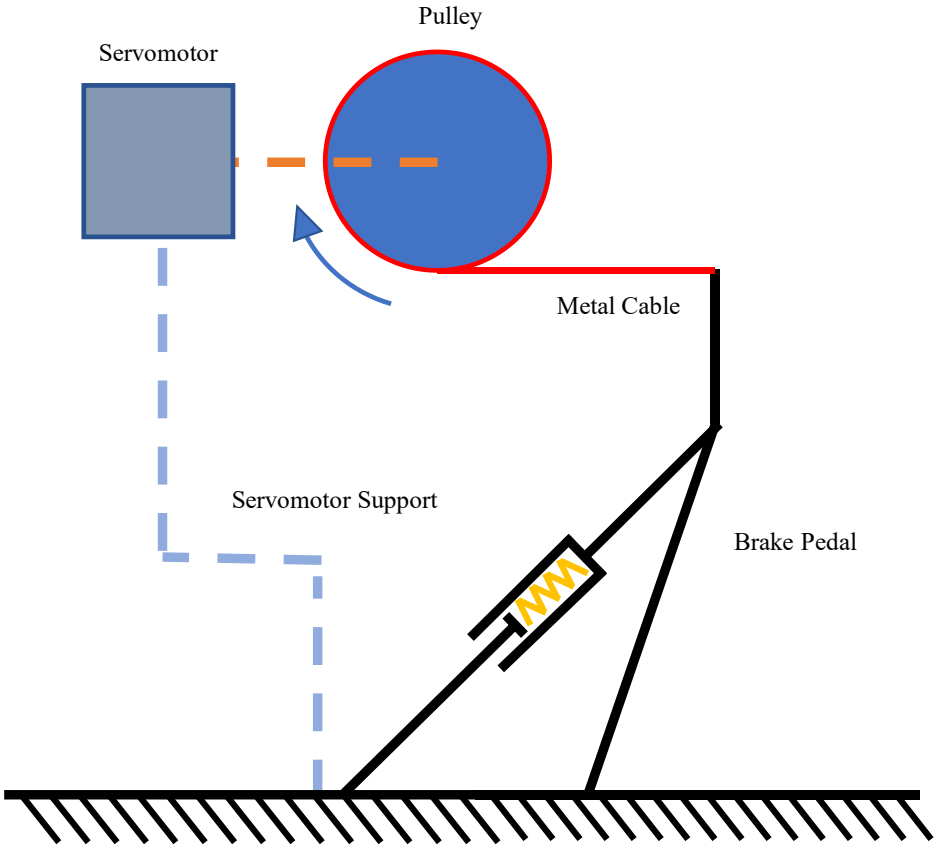

Figure 13 Pedal Actuator Solution

PRO:

- Low cost: all the elements needed to build this device are less expensive compared to other solutions.
- The same hardware in terms of braking line of the already existing system can be used.

CONS:

- Difficult integration inside the monocoque: The system must be placed near to the brake pedal without interfering with other elements or with driver movements.
- Reactants forces between the servomotor structure and the carbon fibre monocoque: some special inserts must be designed in order to integrate this system with the monocoque.
- Control complexity: respect to other solutions, here the rotation of the servomotor is correlated to the arise of pressure inside the braking oil by more complicated equations.

This last solution is the one chosen for this thesis. The reason of this choice is due to the pro and cons highlighted before but also due to the availability of the hardware on the market. All the material needed to build this ASB version were available in time for the competition in Varano de Melegari 2022 and they were compatible with our budget.

Thesis Outline

In the following chapters there will be first a preliminary design of the ASB system, where a simplified 2D model of the system will be done. This model will be useful for a rough preliminary sizing of the components. Then, the parametric multibody model will be presented, and some look up tables to correlate the PWM control signal of the servomotor to the pressure inside the braking lines will be done. Once the control of the chapter will be complete, the design of each component will be shown. In the end there will be the validation phase in which the multibody model with its parametrization will be compared with measured data. After all there will be the conclusions with possible future updates.

Chapter 1 - Preliminary Dimensioning

ASB analytical model

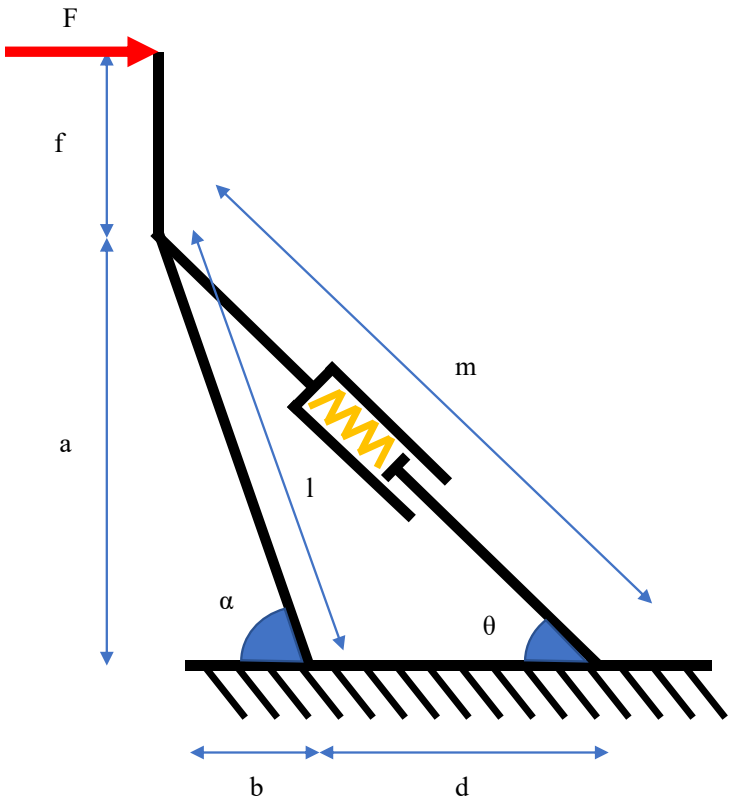

Figure 14 2d simplified model

The aim of this section is to create a simplified analytic model of the manual brake system mounted on the SC19D prototype to find the mathematical function that describes the system kinematic. To do this, some geometrical and physical assumption will be used. First, the system is assumed to be 2D and collapsed on the midplane. Therefore, the balance bar is not considered, and the two independent master cylinders are assumed as an equivalent one.

Through experimental measurement and looking at the datasheet of each component some significant parameters have been found. In the table below the main important parameters useful to describe the braking at this level of approximation are reported:

Spring stiffness	1.3788e+05 N/m
a	0.1276 m
b	0.0702 m
d	0.0501 m
f	0.0713 m

Table 2 parameters of the 2d model

Each parameter has been measured in rest position without any preload on the brake pedal.

Looking at the system simplified in this way the following considerations can be done:

- the static equilibrium of the bodies

$$F_{axial} = \frac{F\frac{h}{a}}{\cos\theta'} = k * (m' - m)$$

- the principle of virtual work

$$Fh(\alpha' - \alpha) = \frac{1}{2}(m' - m)^2 k$$

- trigonometric considerations

$$\alpha = \cos^{-1}\left(\frac{m^2 - l^2 - d^2}{2ld}\right)$$

Considering the diameters inside the master cylinders an evaluation of the maximum pressure corresponding to the maximum pedal displacement has been done. In order to simplify the calculations, the brake, the braking lines, the braking oil and the calipers have been modelled as equivalent springs. The stiffness of the equivalent springs is:

$$k_{oil} = \frac{\max oil\ load}{\max spring\ variation}$$

If we consider this assumption, we can use the previous equations to create a function that links the force needed at the top of the pedal to the brake oil pressure and another one that links the brake oil pressure to the pedal angle alfa (α). Below the plots of these two function done using MATLAB® are shown.

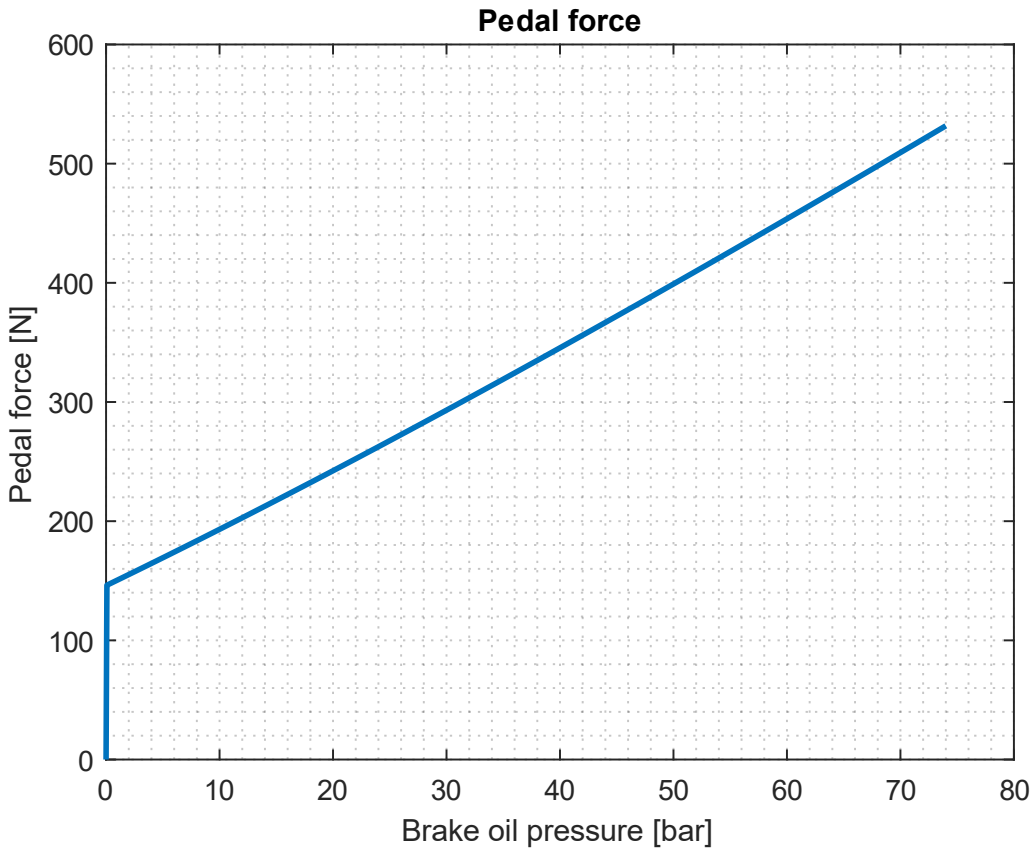

Figure 15 Pedal force vs Brake oil pressure

In Figure 15 at Brake oil pressure equal to 0 the Pedal force has an offset on the y axis. This is due to the presence of the spring preload inside the master cylinders needed to return the pedal to its original position when it is not pressed.

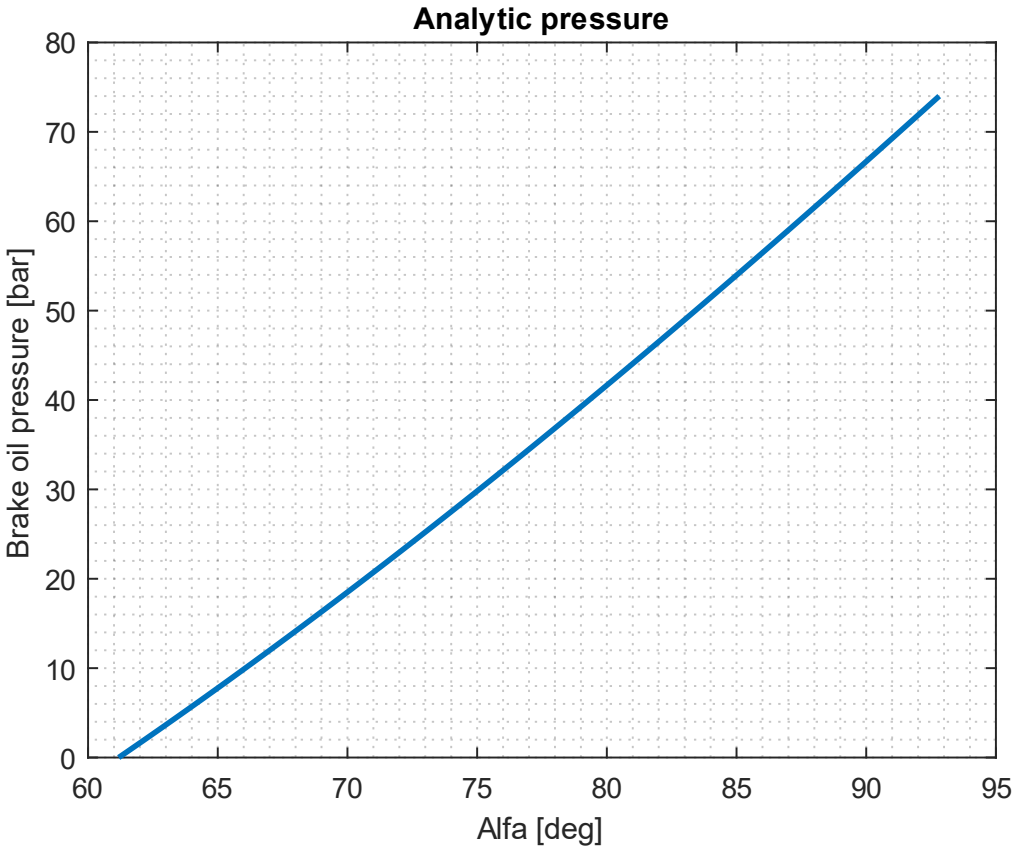

Figure 16 Brake oil pressure vs pedal angle Alfa

As shown in the introduction chapter the target pressure (P_{target}) that the ASB must achieve is 25 bar. Using The function shown in Figure 5 is possible to find the force needed at the pedal top. This force is equal to 267.7 N, so an electromechanical actuator able to apply this amount of force is needed. The spaces available inside the cockpit is low, so a compact solution is needed. Looking at the solutions on the market the servomotor HS-1005SGT has characteristic appropriate to our design and our budget needs.

Figure 17 Picture of the servomotor HS-1005SGT

Below are reported the specifications concerting the servomotor HS-1005SGT [24].

Voltage range	11.1V-14.8V
No-Load Speed (11.1V)	0.26sec/60º
No-Load Speed (14.8V)	0.19sec/60º
Peak current request	6.5 A
Stall Torque (11.1V)	8.24 Nm
Stall Torque (14.8V)	10.79 Nm
Weight	310g
Max rotation	139º
Travel per µs	0.099º/ µs
Max PWM signal range	800-2200 µs

Table 3 HS-1005SGT specifications

The servomotor can develop different torque levels depending on the level on the voltage and the current with which it is powered. In order to develop 25 bar of pressure inside the braking lines, as shown before, a force equal to 267.7 N is necessary. This force in first approximation is considered to be perpendicular to the pedal in order to develop the maximum moment respect to the pedal base joint. The torque that the servomotor must develop to generate a force equal to 267.7 N along the metal cable is directly proportional to the radius of the pulley:

$$T_{SM} = Fr_p$$

Where:

- T_{SM} is the torque generated by the servomotor.
- F is the force along the metal cable that is applied at the top of the pedal.
- r_p is the radius of the pulley.

Form the previous equation is evident how if the radius is higher, also the torque must be higher to generate the same amount of force. So, the pulley should be as small as possible. Anyway, smaller is the radius of the pulley and higher is the angle of rotation of the servomotor for the same length of coiled cable. As a good compromise the radius of the pulley has been chosen as:

$$r_p = 0.025\ m$$

Now, starting from the data of the servomotor shown in Table 4, the force developed by the servomotor to the cable is calculated in each voltage case:

$$\frac{8.24\ Nm}{0.025\ m} = 329.6\ N$$

If the servomotor is powered with a voltage of 11.1V

$$\frac{10.79\ Nm}{0.025\ m} = 431.6\ N$$

If the servomotor is powered with a voltage of 14.8V.

In both cases the force available is enough to generate the pressure of 25 bar inside the braking lines and so to guarantee at least a deceleration equal to 4 $^{m}/_{s^2}$ required by the regulation. The power supply present on the SC19D is sufficient to give to the servomotor 14.8V and to provide the current needed in each situation.

Chapter 2 - Multibody Model of the ASB system

The ASB system is composed by multiple elements that exchange forces and torques between each other. Due to the multiple joints present in this mechanism, during motion the kinematic of each element is three dimensional and complex to predict. An exact equation of the system kinematic would be too difficult to write so, to model the system fidelity to the real brake, a multibody model of the Autonomous System Brake has been developed. A multibody model is a model representation of a system that considers the presence of each element that composes it. Each body inserted in this type of model can have specific properties like weight (to better represents the real inertia), it can be rigid or it can be flexible. Between each element there can be joints and constraints and at each node is possible to apply external forces and torques that physically represents the actual conditions of the system. A multibody model allows to study the dynamic behaviour of each body having a good representation of the system that the model reproduces [25].

In this thesis a multibody model of the whole brake pedal system is developed. The results obtained by the system simulations allow to understand the interaction between the rotation of the servomotor and the pressure increase inside the braking lines. On these results the control of the system will be based. The entire model has been developed on MATLAB Simulink® using the add-on $Simscape^{TM}\ Multibody^{TM}$ [26]. The dimensions of the model are completely parametrized, so is possible to apply any geometrical and physical changes to the model just modifying the script's parameters. Thanks to this feature, during the actual system realization if something is not feasible and must be changed, it is enough to run again the model with the new parameters to obtain a new simulation of the system kinematic. The components that represent the actual ASB system have been schematized in order to make the simulation computationally lighter. Anyway, the actual geometries and proportions have been kept unchanged to better represent the actual system. In the next section a schematic representation of the $Simscape^{TM}\ Multibody^{TM}$ system is shown.

Figure 18 shows the elements chosen to simulate the ASB system. In the picture are highlighted the brake pedal, the servomotor that rotates solidally with the pulley, the metal cable, the servomotor support and the balance bar substystem. This last is shown in Figure 19 in order to keep the sheme clean. All the elements are connected to the same ground that is representative of the vheicle chassis.

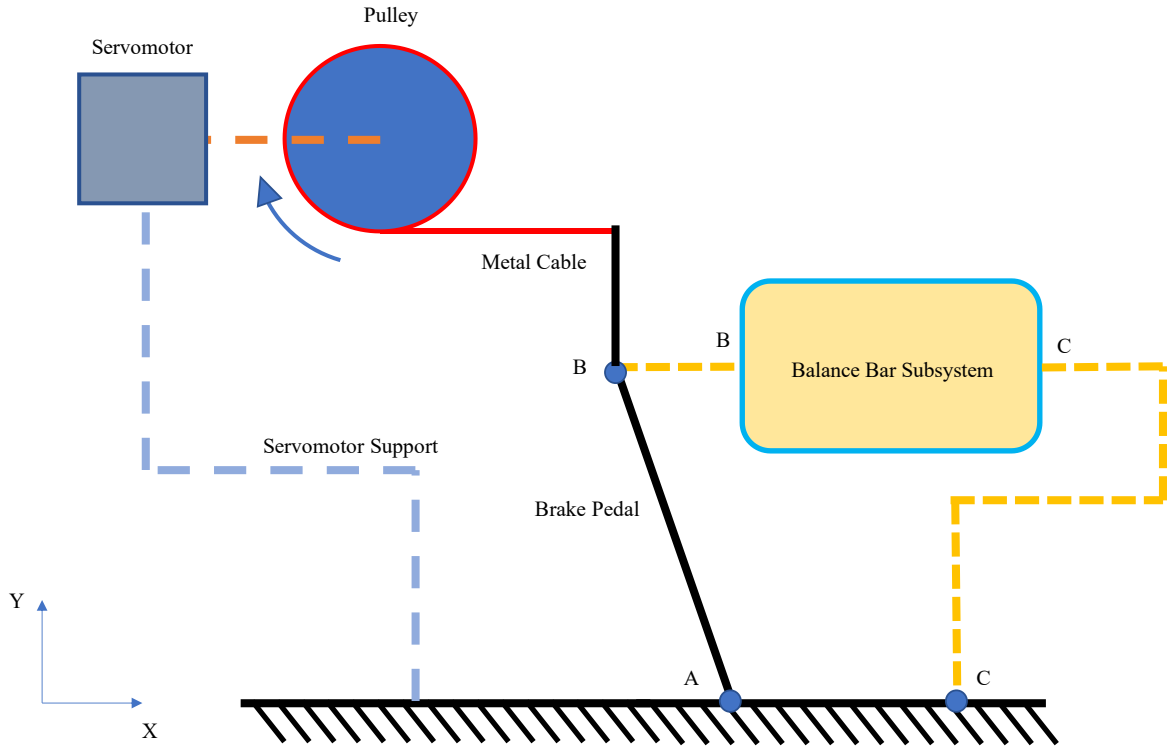

Figure 18 Autonomous System Brake Multibody Schematization

The blue dots in Figure 18 named with letters represent the mechanical joints. They allow the following degrees of freedom:

- A allows only rotation about Z.
- B constraints all the degrees of freedom.
- C allow only rotation about each axle.

As represented in Figure 18, the brake pedal is composed by a rigid body that is hinged to the ground with the joint A at its bottom extremity. On the other end the brake pedal is connected to the metal cable, in that way the metal cable can generate a moment with respect to the pole A. The brake pedal is then attached to the balance bar. The subsystem composed by the two master cylinders and the balance bar have been modelled in the multibody system. A schematization of the model is reported in the Figure below.

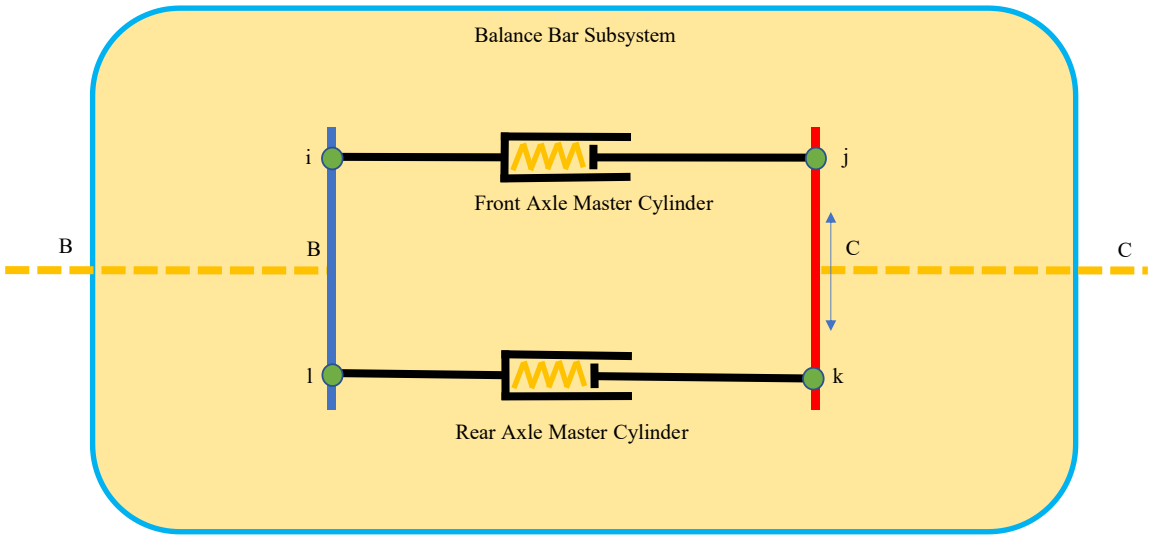

Figure 19 Schematization of the multibody balance bar model

Where:

- i,j,k,l are joints that allows the rotation respect to each axis.
- C can slide along the arrow direction to change the effort between the front and the rear line of the balance bar during braking.
- The master cylinders are represented by two prismatic joints linked in parallel with springs.

In order to model the master cylinders, the compliant elements are assumed as the sum of two contributions: the contribution of the spring inside the master cylinder plus the equivalent compliance that represents the reaction force due to increase of pressure inside the braking lines during master cylinder's piston displacement.

Below a capture from the model realized on $Simscape^{TM}$ $Multibody^{TM}$ with the actual geometries of the real system is reported.

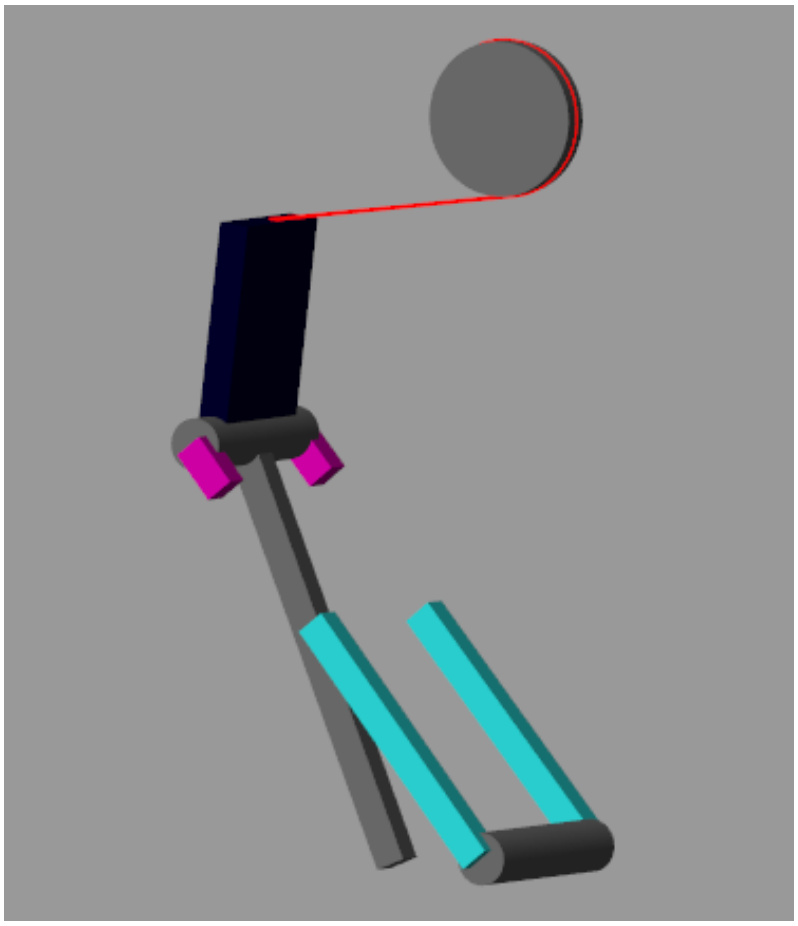

Figure 20 ASB system modelled in Simscape™ Multibody™

The elements in the figure above are really schematized but they represent the real geometries of the most important elements of the real system. The simulation done in *Simscape™ Multibody™* has been used to extrapolates the data of the position of each element during the pedal actuations. Thanks to those results the following correlations have been founded.

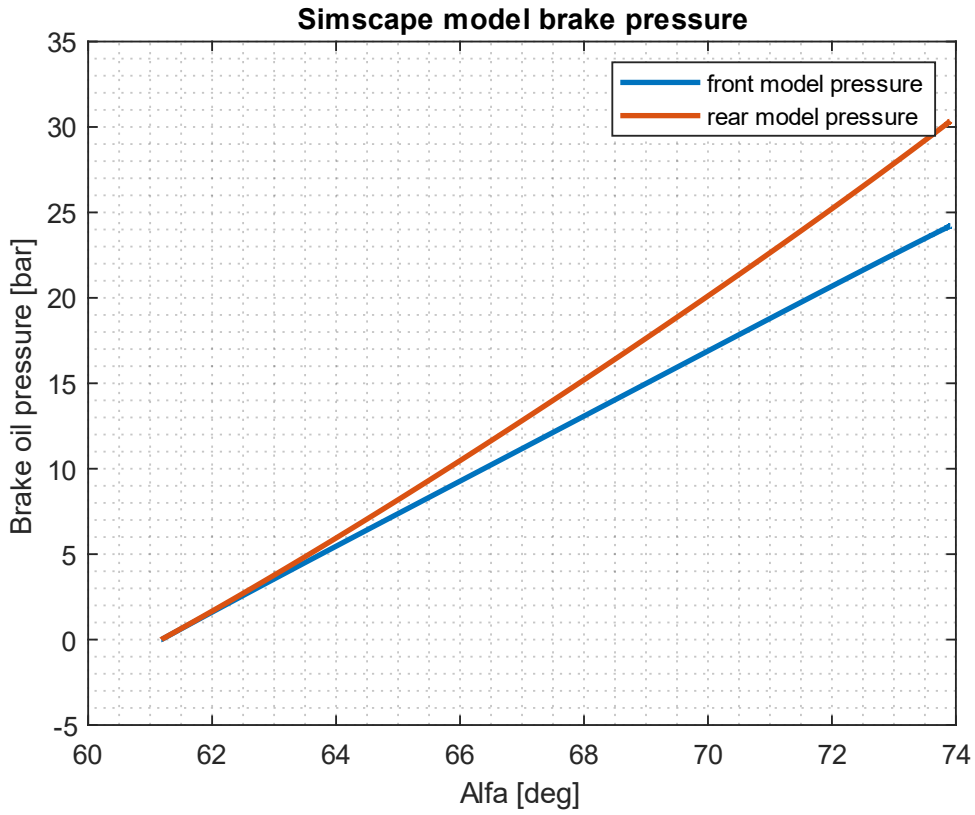

Figure 21 Pressure insider each axle modeled in Simscape

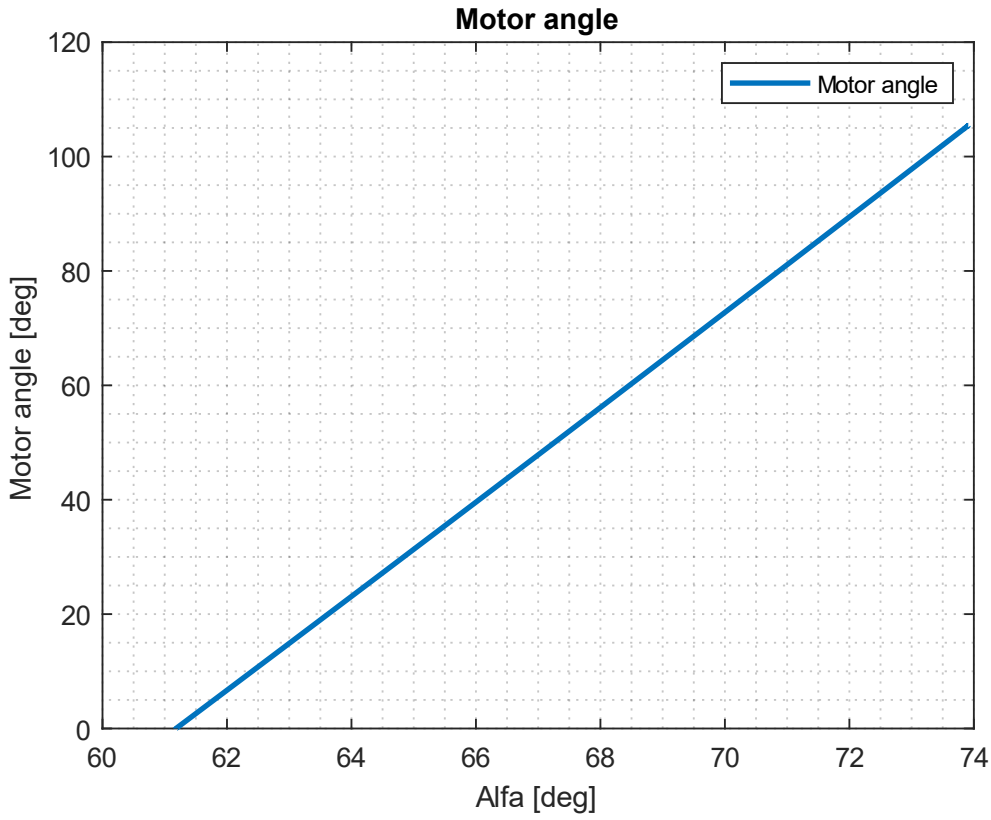

Figure 22 Position of the servomotor depending on pedal position

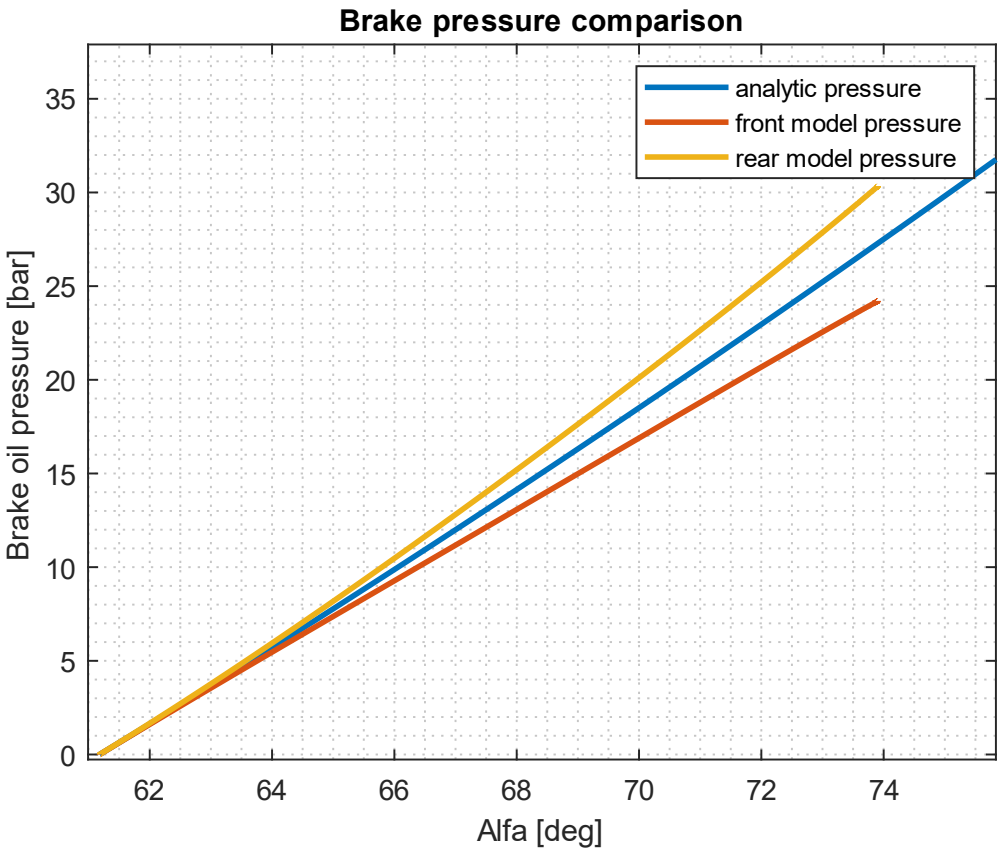

Figure 23

Comparison between the pressure trend in multibody model and the ones obtained in the analytical model

A first validation of the equations used for the 2D model designed in the initial dimensioning can be done with the data obtained with the multibody model. Those data are compared with the ones obtained analytically on the plot shown in Figure 23. The trend between the two model is almost the same except by the divergence behaviour between the front and the rear line. Even if the balance bar is in neutral position, due to the different internal diameter between front and rear master cylinders, the partition is moved toward the rear line.

In order to control the system, with the data obtained above the following relation between the motor angle and the brake pressure is obtained.

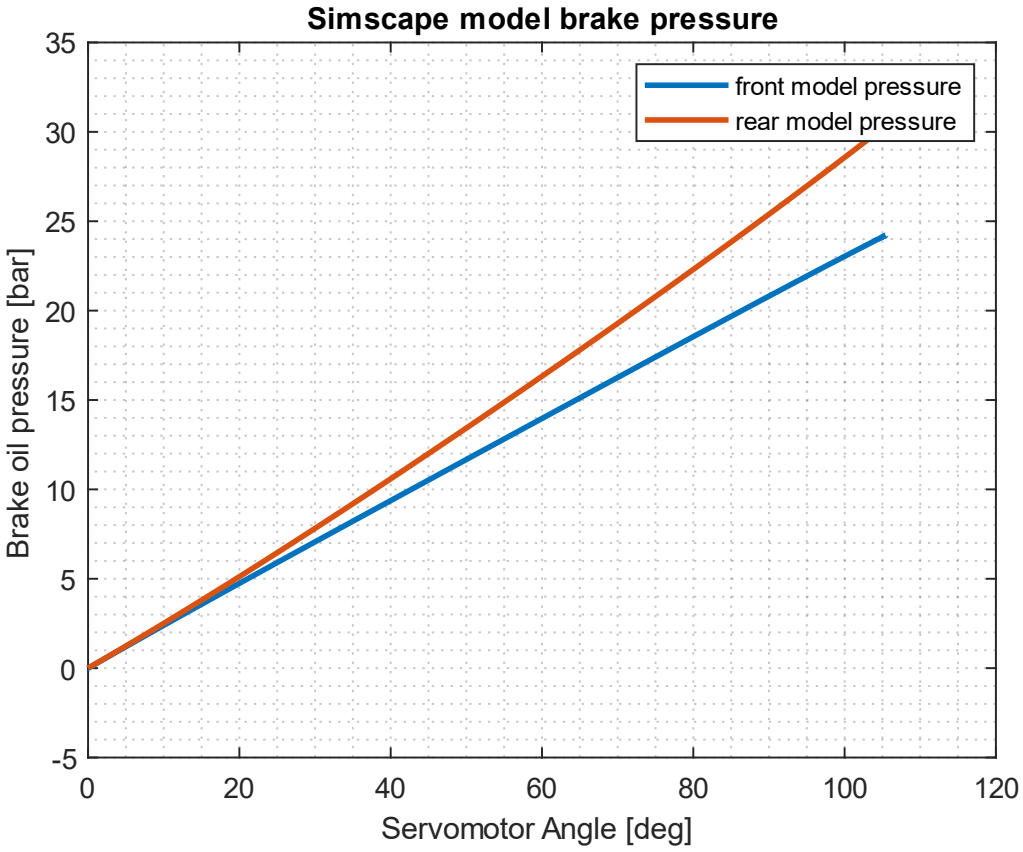

Figure 24 Brake pressure inside each line in function of the Servomotor angle

Chapter 3 - System Control

The aim of this section is to design a control for the autonomous system brake that can actuate the system in order to keep the pressure at a desired level. The idea is to develop a low-level control that satisfies the request sent by the high-level control of the board dedicated to the path planning. The control will be developed on lookup tables derived by the multibody simulation. A PID controller will be developed to modulate the servomotor PWM signal in order to reduce as much as possible the error between the desired brake pressure and the effective brake pressure inside the brake line.

Lookup tables

A lookup table is "an array that replaces runtime computation with a simple array indexing operation" [27]. To control the system a lookup table of the function that links the servomotor angle to the brake oil pressure has been defined starting from multibody simulation data. In this way, if a certain amount of pressure is demanded, the lookup table can directly convert it into a request of target angle for the servomotor in form of PWM signal. The two braking lines are differentiated and on each of them there is a pressure sensor. Since the system is developed in a way that if the balance bar is positioned in neutral position the rear line reaches higher pressure, the control is done only on the front brake line that is the one with lower pressure. In this way at least a certain amount of pressure is guaranteed on both lines. The logic behind the lookup table for this application is highlighted in the figure below. The data shown in this plot are the ones obtained by the multibody simulation. It is important to remember that, anyway, if the calibration of the balance bar is changed, thanks to the parametrization of the multibody model each lookup table can be computed again.

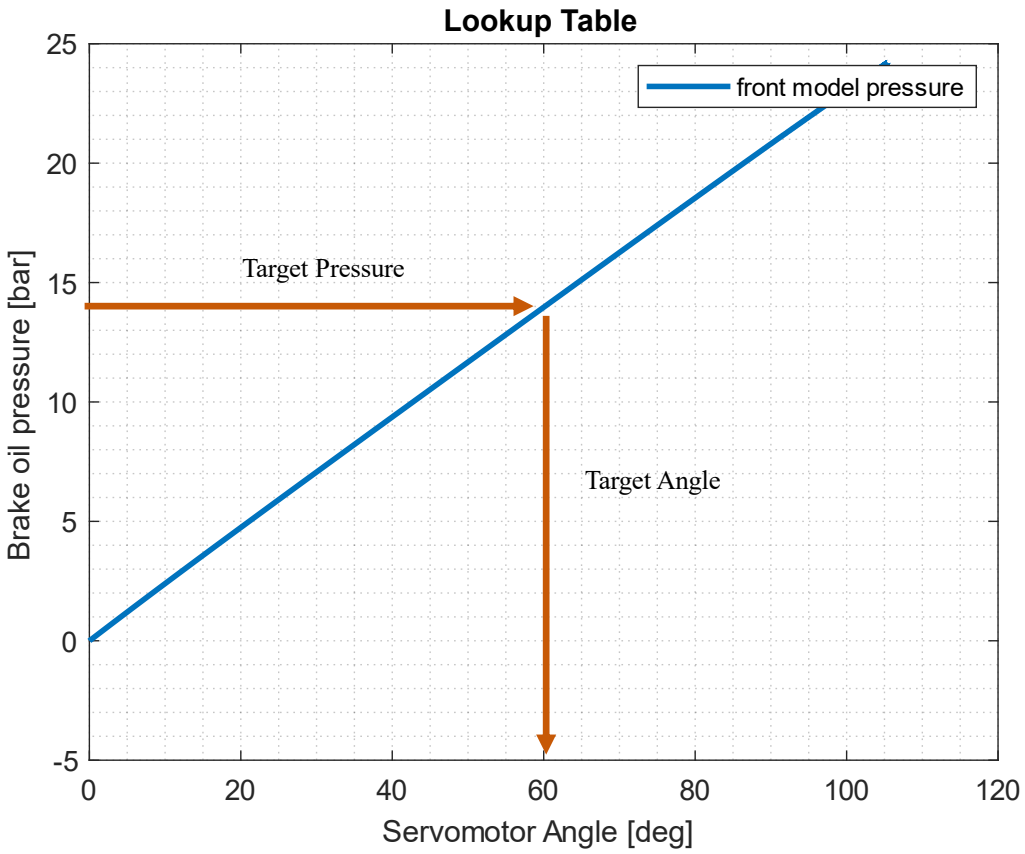

Figure 25 Lookup table example

In Figure 25 there is a graphical example of the operation that the logic on the ASB control does in order to convert the target pressure coming from the path planning request in a target angle for the servomotor. To understand how to manage the servomotor control is useful to understand before its working principle [28].

In servomotors there are usually three electric inputs:

- A ground.
- A positive input.
- A control input in which the PWM signal is sent.

The PWM of a servomotor is a signal with a frequency and a duty cycle that indicates to the internal servomotor board which is the position that it must assume. For the servomotor HS-1005SGT the PWM range is 800-2200 µs for a motion range of 139º. It means that if on the control input a signal that has voltage equal to 5V and the duration of 800 µs is sent, the servomotor will go on the initial position (angle equal to 0º). If instead the duration of the signal is 2200 µs, the motor will rotate up to a motor angle

equal to 139º. To reach intermediate positions, a linear interpolation must be performed following the equation below.

$$\tau = 800 + \frac{2200 - 800}{139} * \beta$$

Where:

- τ is the pulse width corresponding to the target angle.
- β is the target servomotor angle.

Thanks to this relation is now possible to directly link the pressure target sent by the path planning not just to a motor angle but to a PWM signal. This signal can be sent to the real motor in order to control it and so starting to link the results obtained by the model to the real system.

Open loop control

The control designed starting from the data obtained by the model and its lookup tables allows to link the PWM signal to the pressure inside each braking lines. Anyway, if in the system there isn't any feedback about the control's effectiveness, this is an open loop control. The schematization of the open loop controller is shown below.

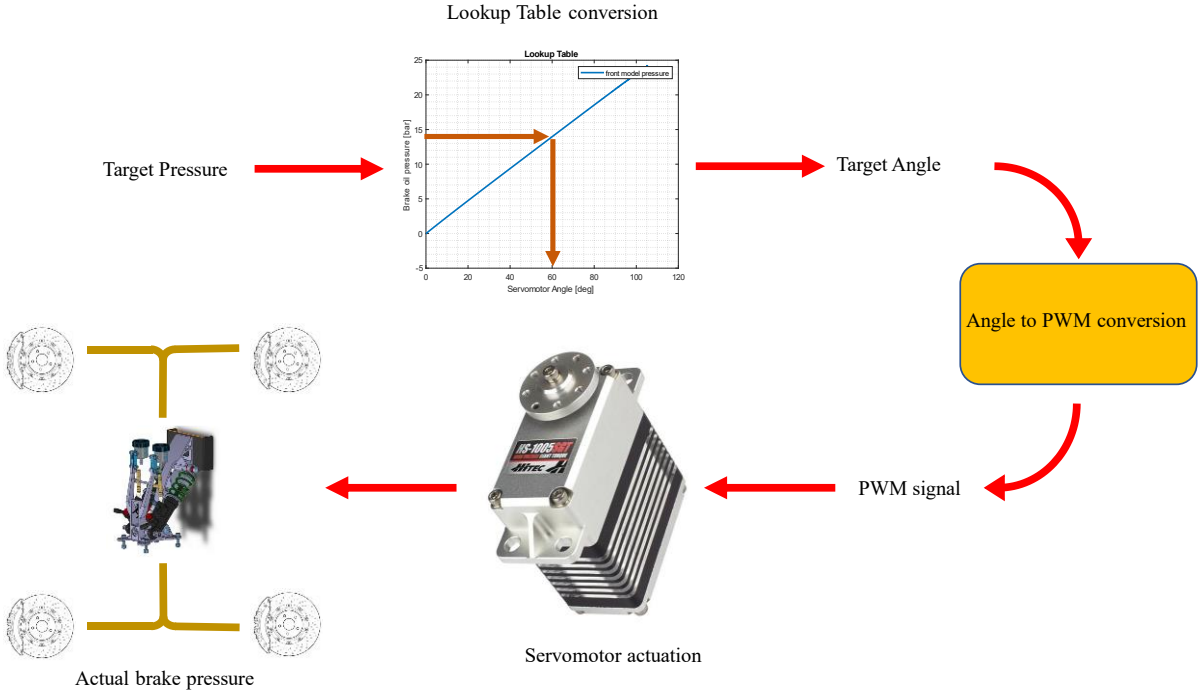

Figure 26 Schematization of the open loop control

With this type of controller during the actuations is not possible to understand if the target is effectively satisfied by the system, so a closed loop controller has been designed.

Closed loop controller

The idea of this controller is to use the pressure sensor on the front brake line to detect which pressure is actually present inside the system and use it as feedback to calculate an error compared to the target pressure. The controller designed in this section is a PID controller.

A PID controller is a simple controller born at the begin of the last century [29] that takes into account the past, the present and the future in order to control the system. The classic formulation in the continuous time domain is the following.

$$u(t) = K_P e(t) + K_I \int_0^t e(\tau) d\tau + K_D \dot{e}(t)$$

Where:

- $u(t)$ is the controlled input of the system
- $e(t)$ is the error between an actual signal and its reference
- $K_P e(t)$ is the proportional factor that depends on the constant K_I. It provides a gain that depends on the current error and so it must be properly chosen since if it is too high it will provide big oscillations and if it is too low it will make the controller less effecting.
- $K_I \int_0^t e(\tau) d\tau$ is the integral factor. It provides a gain depending on the constant K_P that increase the effort of the sum signal in previous instants. Higher are the past errors and higher will be weight of the integral in this formulation.
- $K_D \dot{e}(t)$ is the derivative factor. It depends on K_D and it is related to the slope of the error.

The controller developed for the ASB system is schematized in the following figure.

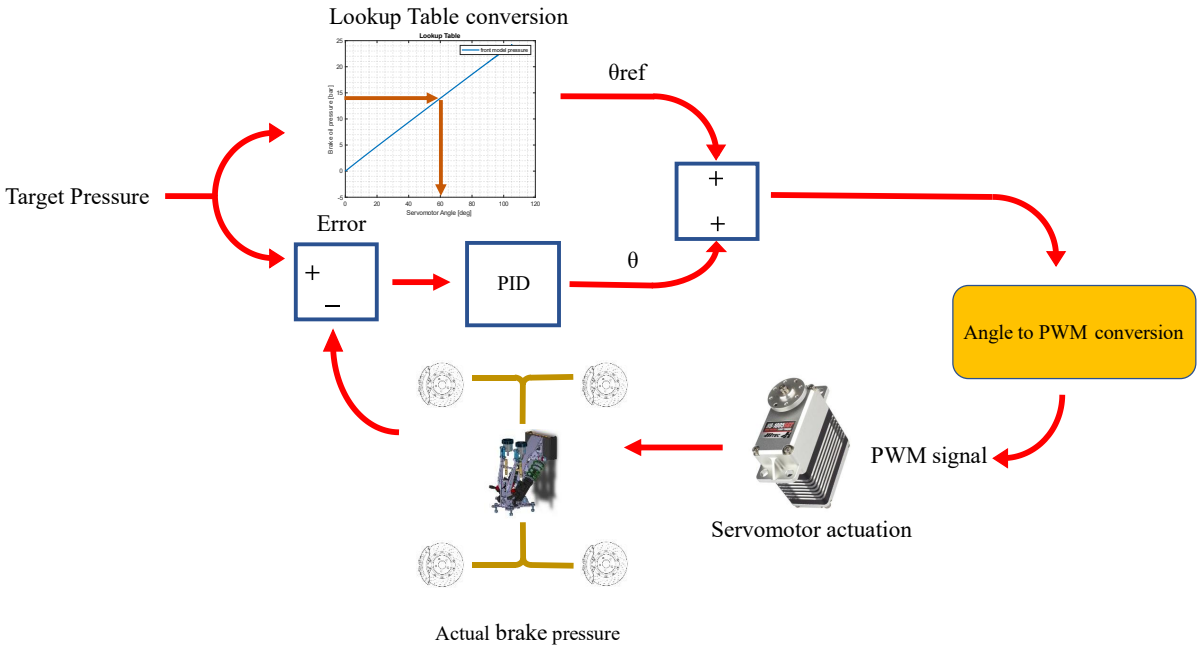

Figure 27 Closed loop controlled system

PID controller development

In order to satisfy the pressure requested by the path planning, a low-level closed loop controller has been developed for the ASB system. The controller designed is a PID and to define it the constants K_P, K_I and K_D must be found. The design of this controller has been performed on the simulated system developed on $Simscape^{TM}$ $Multibody^{TM}$ with a trial-and-error approach. The idea is to use the digital twin of the actual system realized in the sections before coupling it with a simulated Servomotor with the same characteristics of the real one and a PID controller that reduces the simulated error. Once the PID parameters will be defined, they will be used and tested on the real system. The optimal PID parameters founded for this application are:

- $K_P = 0.01$
- $K_I = 3$
- $K_D = 0$

Since the value of K_D is zero, the obtained controller is a PI and not a PID. During tests both on the vehicle and on the model, choose a null K_D used to lead to a more stable transient dynamic with less oscillations. The results of the controlled system are shown in the following plots.

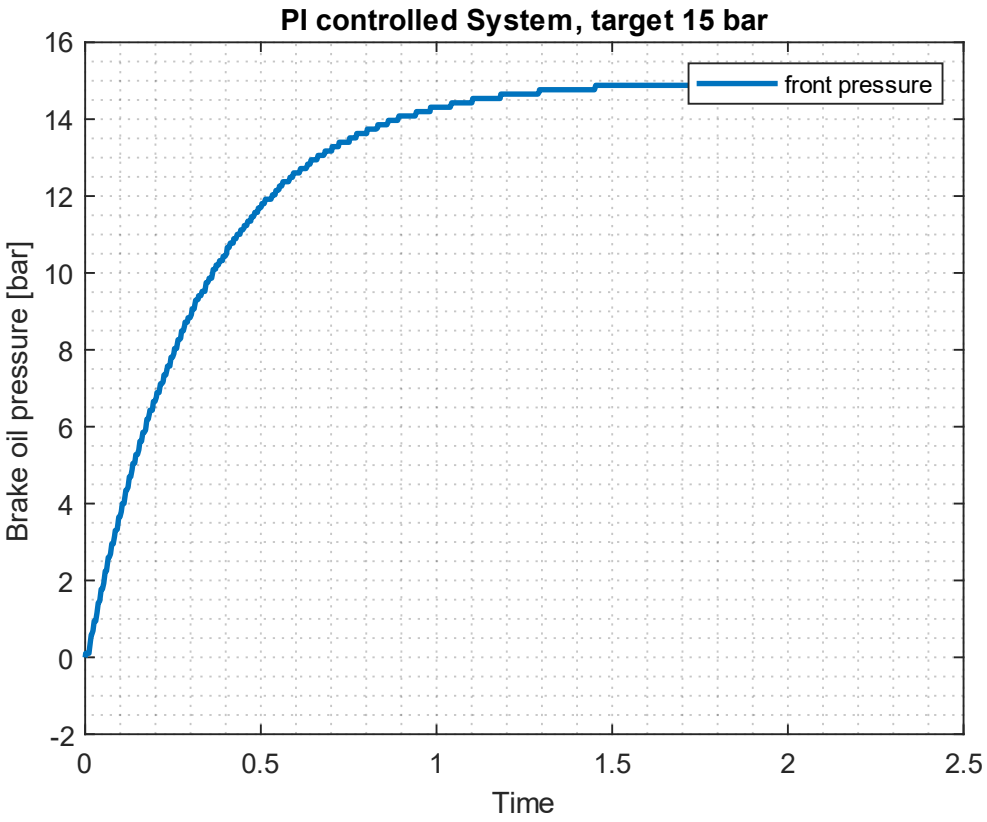

Figure 28 brake oil pressure in the simulated model with a PI controller

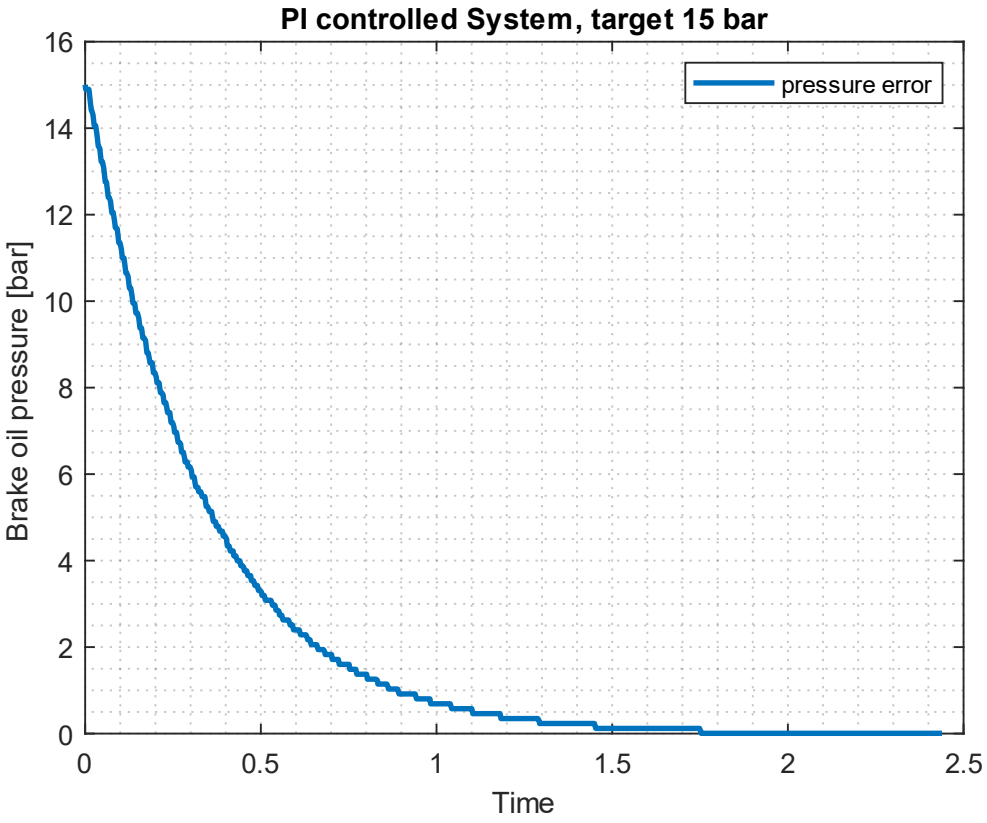

Figure 29 pressure error in the simulated model with a PI controller

The plots above represent a simple test in which a target pressure is demanded, and the servomotor actuates the pedal to satisfy the request. The PI controller shows a good behaviour reaching the value in less than 2 seconds and without any oscillations around the steady state value.

Chapter 4 - Mechanical implementation

The integration of the system inside the cockpit was one of the most crucial points during the system design. The Formula Student regulation imposes that the autonomous actuators must not interfere with the space deserved for the driver. In this case the location of the actuator is near to the brake pedal and so it must allow the correct legs and feet movement for the driver. For this reason, the system has been located behind the pedal with a mechanical support studied in order to attach the motor at the top part of the carbon fibre monocoque. This position doesn't interfere with any driver movement. Moreover, the location has been studied also to guarantee an easy maintenance during the sages of the competition or during tests.

ASB support

To fix the system at the desired position inside the cockpit, a support has been developed. The target in its dimensioning were the one to don't interfere with the system movement, the facility in the installation and to have enough mechanical strength. In the following section the 3d cad model and the FEM analysis result of the final support design are reported.

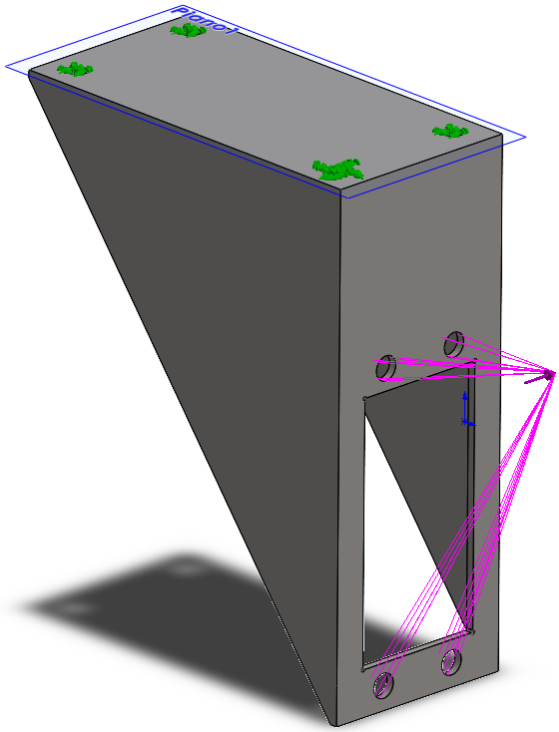

Figure 30 ASB support

The material of the support is common steel and it is realized with cut and welding. The numerical analysis done on this support are static in the following conditions.

Load Type	Magnitude	Direction
Force	600 N	Steel wire direction
Constraints	Fixed	6 D.o.F.

Table 5 Support Numerical Analysis description

The magnitude of the force has been evaluated in the worst load condition. For the constraints there is the assumption that the support is attached to an infinitely rigid structure. It is not true since the carbon fibre is less stiff than the steel support, and so when the load is transmitted by the steel wire cable the monocoque should deform. Anyway, for the purpose of this test this assumption is good since considers a limit case and so give us a further safety factor on the static analysis result.

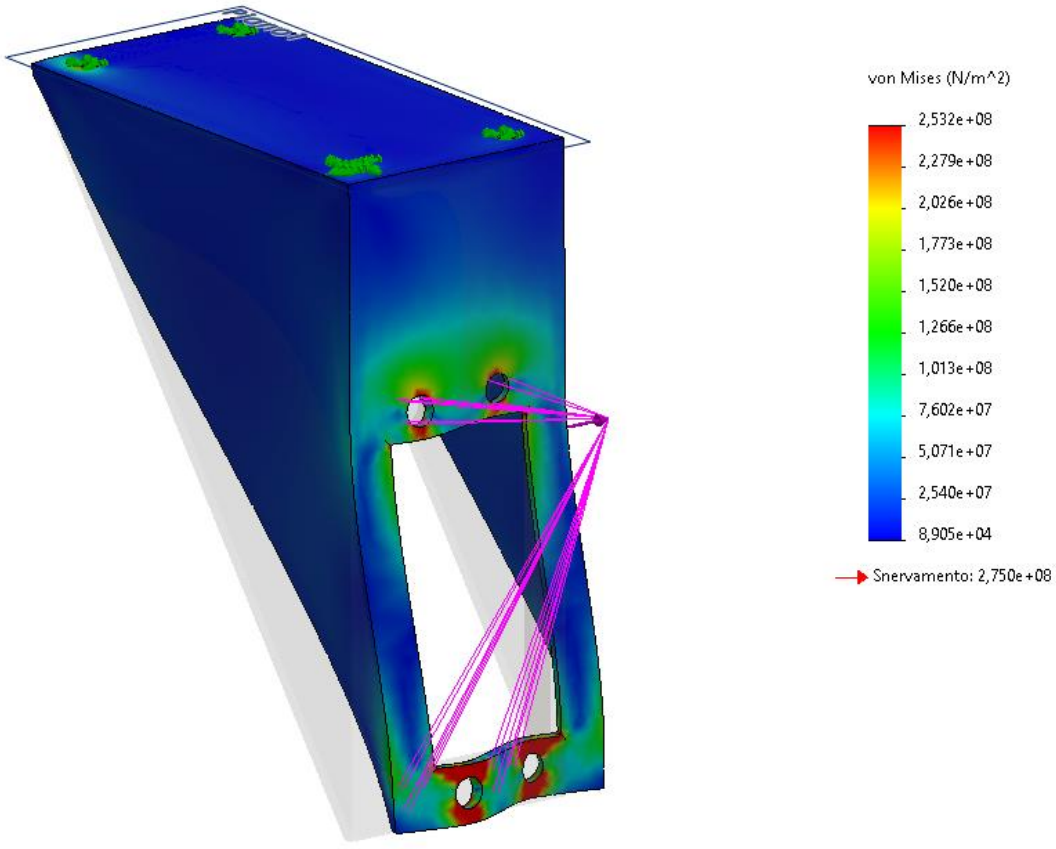

Figure 31 Von Mises Stress, deformation scale 44,89

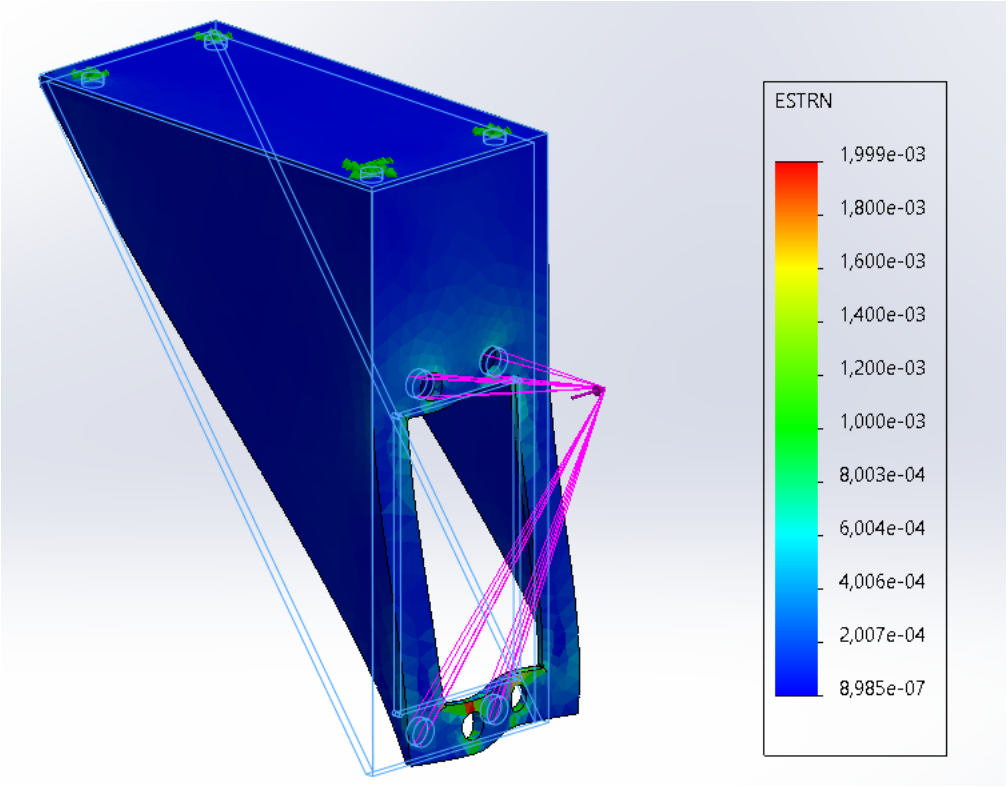

Figure 32 Equivalent Strain, deformation scale 44,89

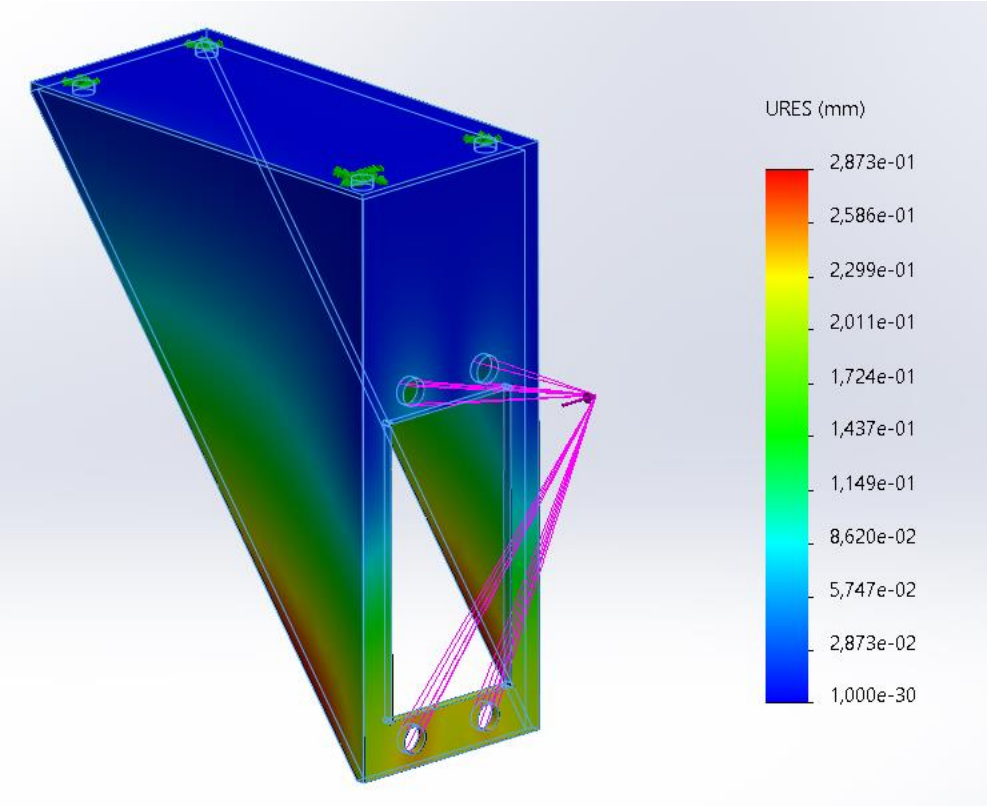

Figure 33 Displacements, deformation scale 1

The maximum force along the cable evaluated in Chapter 1 – Preliminary Dimensioning were 267.7 N, so considering a force equal to 600 N allows to keep a good safety margin. The results of the static numerical analysis prove that this geometry combined with the steel are a good choice for the realization of the support for the ASB. To mount this support without have local rise of stress in any point of the carbon fibre that could damage it, some special inserts have been designed. The aim of these support is to distribute the pressure due to the autonomous brake actuation on the monocoque.

Motor Pulley

The interface between the servomotor actuation and the metal cable is the pulley. It must withstand to the maximum load and its geometry must be properly designed in order to have the correct motion of the cable during its rotation without any misalignments of the cable.

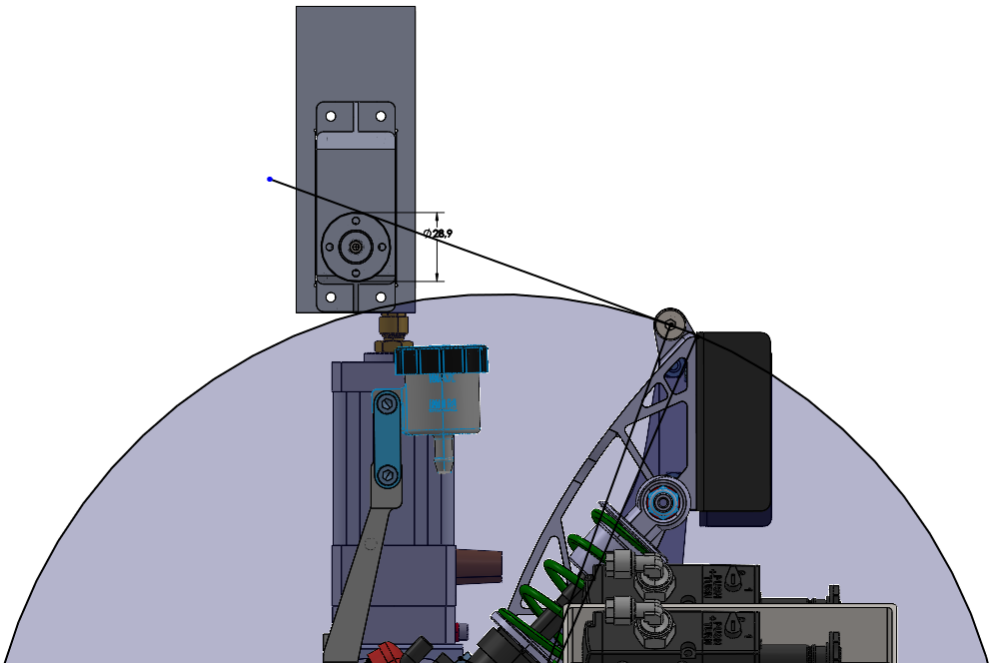

Figure 34 Assembly of ASB system

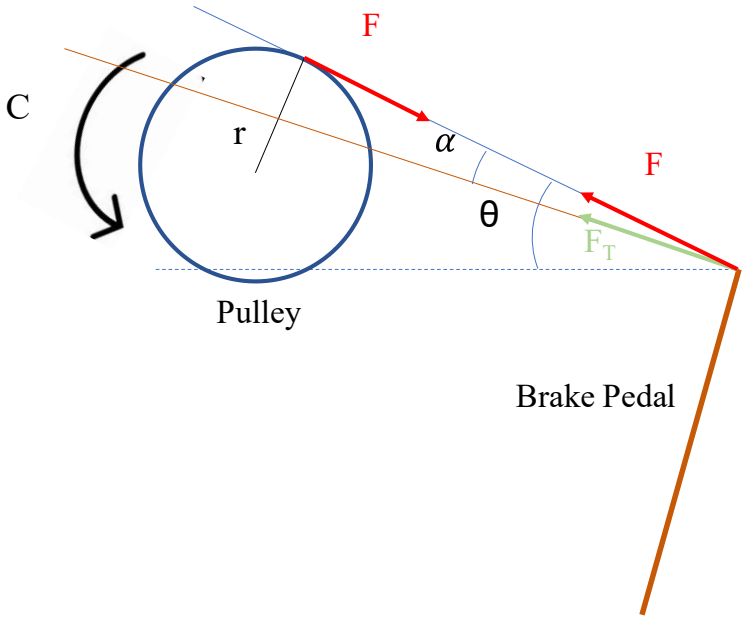

Figure 35 Motor Pulley Force Evaluation

Where F is the force along the metal cable and F_T is the force perpendicular to the brake pedal that can develop the maximum amount of torque. During the motion of the pedal the inclination of the cable with respect to the brake pedal changes increasing o reducing the actual effort. The following physical and mathematical considerations can be done.

$$F = \frac{C}{r}$$

Where C is the torque of the servomotor and r is the radius of the pulley.

$$F_T = F \cdot \cos(\alpha) = \frac{C}{r} \cdot \cos(\alpha)$$

$$\alpha = \alpha(r)$$

Where α is the angle between the direction of F and F_T. Higher is this angle, lower is the force perpendicular to the brake pedal and so the effort that the servomotor can apply on the brake lines.

The design of the pulley has been developed in order to be able to wind the cable for at least 180 degrees. Below is reported the final design.

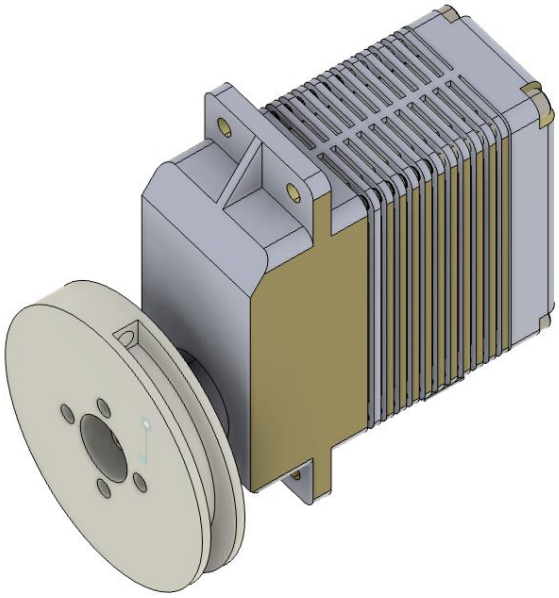

Figure 36 Assembly of the servomotor with the pulley

The realization of this component is done with an FDM additive manufacturing machine to have the possibility to recreate topological optimized shape limiting at the same time the costs. The material chosen is ABS (Acrylonitrile butadiene styrene) that is one of the materials with best mechanical characteristics. The realization of this component in steel would require a too high budget and long production time so the choice of ABS was the more convenient. Due to the production process of the FDM additive manufacturing the component are not so strong in traction because the layer could tend to divide one from each other. Due to this reason this component has been designed in order to be printed with the main axis perpendicular to the printer plate and the hole for the cable has been designed in a way that the force that act on the pulley during braking actuation doesn't pull the material in the contact area, but it compresses it. Here are reported the FEM analysis performed on the component. In order to be coherent with the numerical analysis performed on the support, the force applied on this component is equal to 600 N and always directed in the same direction of the metal cable.

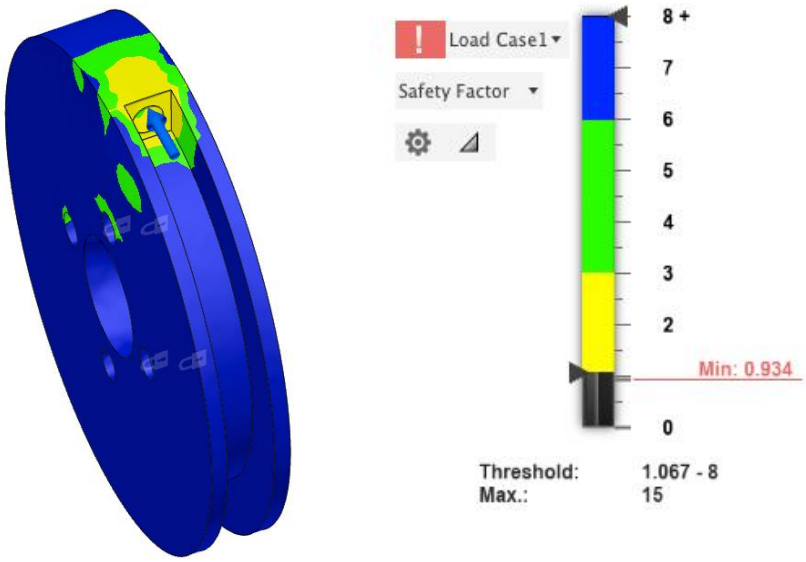

Figure 37 Pulley FEM analysis results

The results show that there is a singularity point in which the safety factor goes slightly below 1, anyway the load case considers intrinsically a safety factor since the applied force is 600 N but the maximum estimated one is just 267.7 N. During tests this approach seemed to be good for this application since the component never showed any weakness and thanks to FDM even if a little modification were necessary, it was easy to produce in short time another version of the component. Below some pictures of the real system are reported.

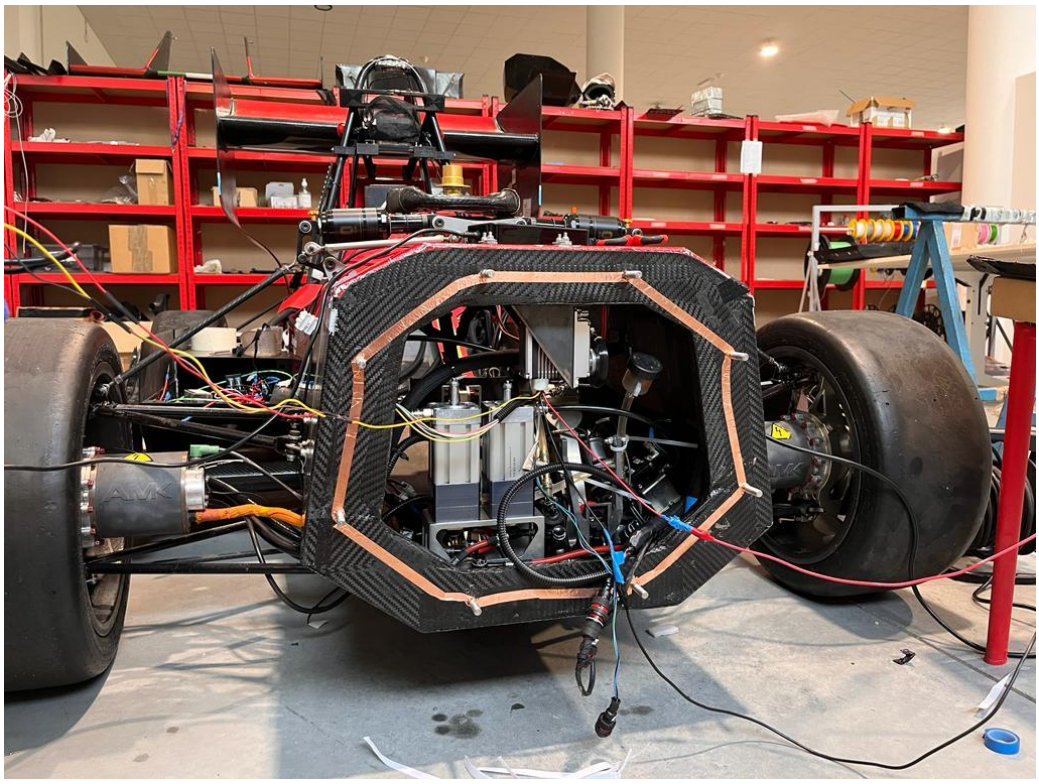

Figure 38 Front of the SC19D with the ASB equipped

Figure 39 Detail of the ASB system seen from the front of the vehicle

Chapter 5 – Experimental Campaign

In this section the logs of the experiments performed on the vehicle and the results are shown. The vehicle is equipped with pressure sensors on both the braking lines, so an evaluation of what is happening inside them can be performed. Since the servomotor doesn't give any feedback about its position and there isn't any brake pedal position sensor, the ASB can be seen as a black box that receives some PWM signals and gives a certain pressure inside the front and rear lines. The tests proposed in this section are thought in order to give an indication of the system performance and validate the control obtained by the multibody system with its assumptions.

Multibody Model Validation

To validate the multibody model a test that can be done is to perform the same test with the same conditions both on the real and the simulated system and to compare the results. The test that is shown in this section has been performed in open loop, and so without the use of the PI controller, both on the real and the simulated system. The aim of the test is to demand to the servomotor a certain target angle that has step increments and decrements during the time. The test is constituted by a cycle that covers the entire servomotor rotation range. Since the HS-1005SGT can rotate in a range between 0 and 139 degrees, the cycle has been designed with fourteen step increments of ten degrees (except the last one that is just nine degrees), one each second. Once the maximum angle has been reached, the servomotor goes back to the initial position following the same strategy. The reason why the test covers all the rotation domain is to highlight how the differences between the simulated and the real system evolve during the motion.

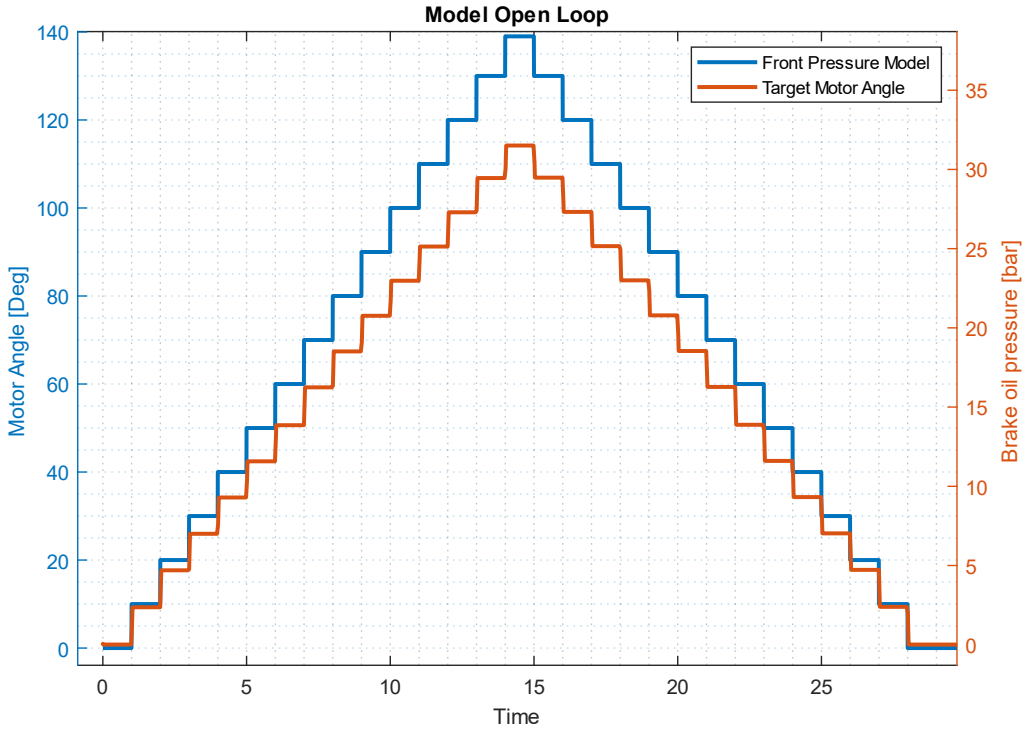

Figure 40 Data from the multibody simulation

In Figure 40 the test cycle is performed on the multibody model. The pressure increases during the time according to the motor angle rotation. The ratio between the motor angle and the pressure inside the lines is almost constant, at each step the increment of pressure is the equal to each other. Another important factor is related to the symmetry between the ascending and the descending behaviour. Below the same test regarding the real system is shown.

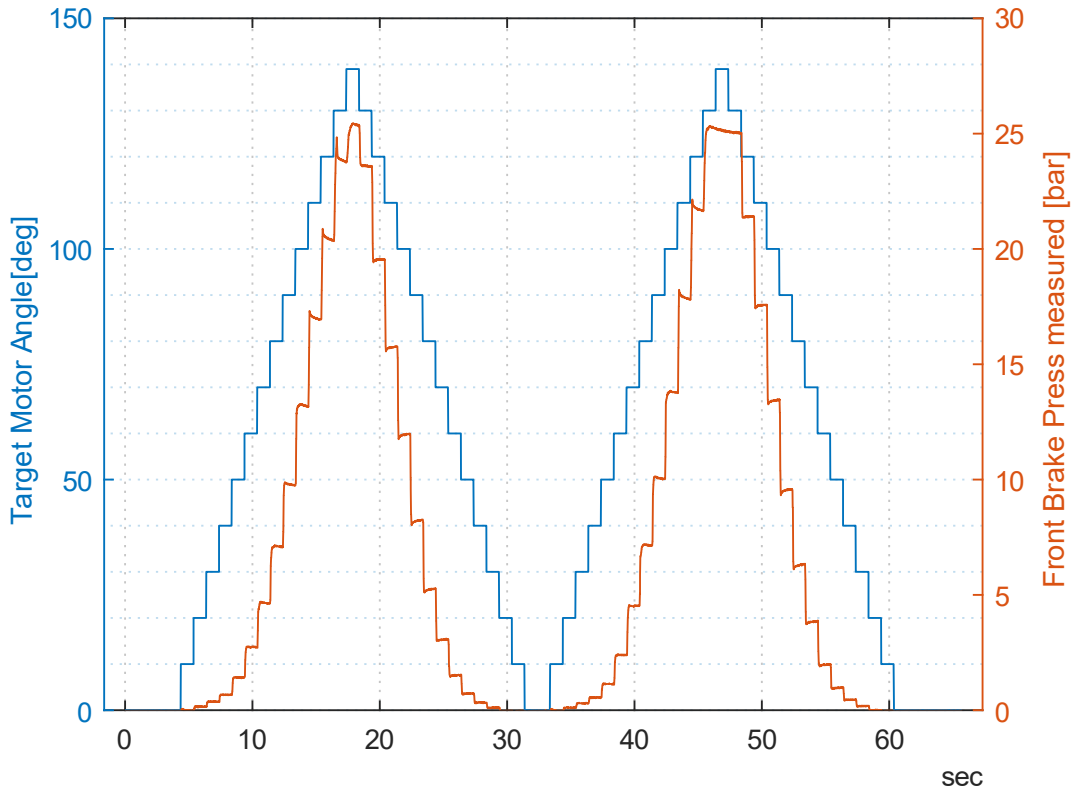

Figure 41 Data from the real test

A big difference between the simulated and the real model is about the information of the motor position. In the simulated system we have the information about the position of the servomotor, while in the real system there isn't any sensor that can detect this value, so in the Figure 41 the plot is only regarding the target position that the high-level controller sends to the ASB system. This means that even if on the plot a certain angle is demanded, there could be the possibility that the servo motor is not be able to provide enough torque to achieve it. This behaviour explains the saturation that incomes at the top of the pressure peaks in the real system experiment: even if a greater angle is asked, the servomotor cannot provide more torque than the one corresponding to about 25 bar of pressure. As visible in Figure 41, between the two cycle there is a certain cycle-to-cycle difference. This is mainly related to the hysteretic characteristic of the servomotor. During tests has been noticed that even if the conditions were the same, the servomotor sometimes provides less torque, especially if it performed an actuation few instants before. This is due to the temperature increase of the servomotor that during actuations generates heat from friction and joule losses.

Looking at the bottom part of the stairs is visible how the increment of pressure is qualitative lower with respect the one after about six steps. This is related to the tension of the metal cable. Since, in order to be simpler, the ASB is not equipped with a cable tensioner, during the rotation of the pulley initially the cable is not in tension and so provides less force to the top of the pedal. After few iterations the system is in tension and so can provide the maximum torque.

An important analogy between the two systems is about the increment at each step and the symmetrical behaviour. As said before, the increments in the bottom part are lower and at the top part are limited by the motor torque saturation, anyway at the middle (from 5 to 25 bar), that is the main operating area of the ASB, the increments are almost equal at each step. In the simulated system, which is free of imperfections, each step is exactly equal to each other. This behaviour is the same of the multibody model. Another factor is related to symmetrical behaviour between the ascendent and the descendent phase. In the real system the differences between the corresponding steps of the ascendent and descendent phases are less than one bar. Moreover, between the two cycles shown in Figure 6, these differences are not always the same. This is due to internal dry friction inside the joints and the master cylinders. The last and evident comparison that can be done about the two experiments is for what concerns the pressure reached at rotation degree between the real and the simulated system. In the simulated system, the pressure achieved is higher and is not corresponding to the real one at each step. This is due to the limitations of the equivalent spring model and due to the lack of information about the servomotor position in the real system. In Figure 40 the target angle corresponds to the actual angle, in Figure 41 is possible only to know the demanded angle but not the achieved one, so the ratio between pressure and angle could be different from the one showed.

A further validation can be done about the model of the balance bar looking at the trend of front and rear pressure at each iteration between the real and the simulated system. The aim of the balance bar is to partializing the effort on the front and the rear braking line by means of an adjustable beam. If the system has been correctly modelled the ratio between the two braking lines should be equal during the brake pedal motion.

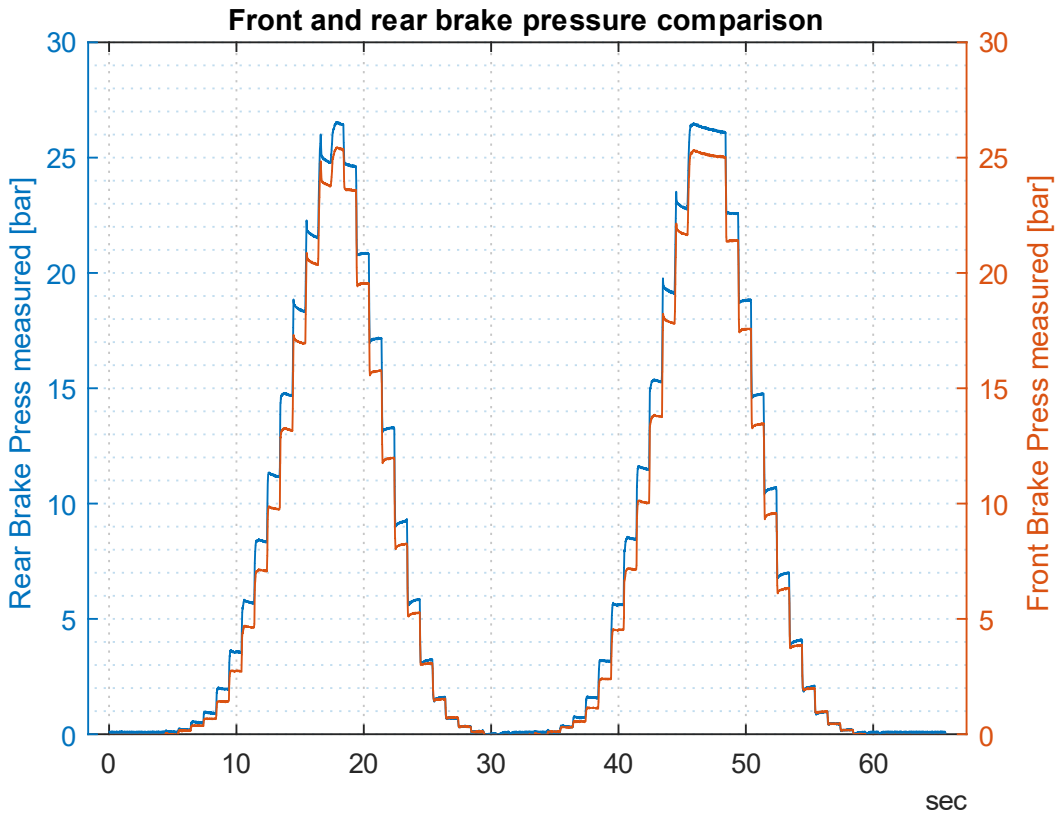

Figure 42 Front and rear brake pressure comparison

The two pressures in both lines increase and decrease together depending on pedal effort. As expected at the beginning, due to the balance bar and the different master cylinder between the front and the rear line, the front brake line reaches higher pressures at each time step. Looking at each step the pressure initially has a spike and then converges to a steady state value. The reason of these spike is due to the maximum instantaneous torque of the servomotor that is higher compared to its continuous torque. The entity of the spikes become higher going closer to the top of the stairs and the time that occurs to reach a steady state value increase. In terms of system dynamic in the open loop behaviour the pressure increases almost instantaneously with a rising time of the order of 0.2 sec. The spike of pressure is also conductible to a shock wave inside the oil that generates when the brake pads impact against the discs. Moreover, due to the hysteretic behaviour and the losses inside the e-motor, after multiple actuations these spikes start to decrease. This changing is visible looking at the different behaviour between the first and the second stair in Figure 42. The step increase of pressure in proximity of the mid working area is about 5 bar, corresponding to 10 degree of servomotor rotation. An almost instantaneous rising time means that the behaviour can be seen in first approximation as a step increase. Since the big pressure gap, the oil inside the braking line is accelerated and it contributes

to the generation of pressure waves. The data collected during the experiment have been elaborated in order to find the following trends.

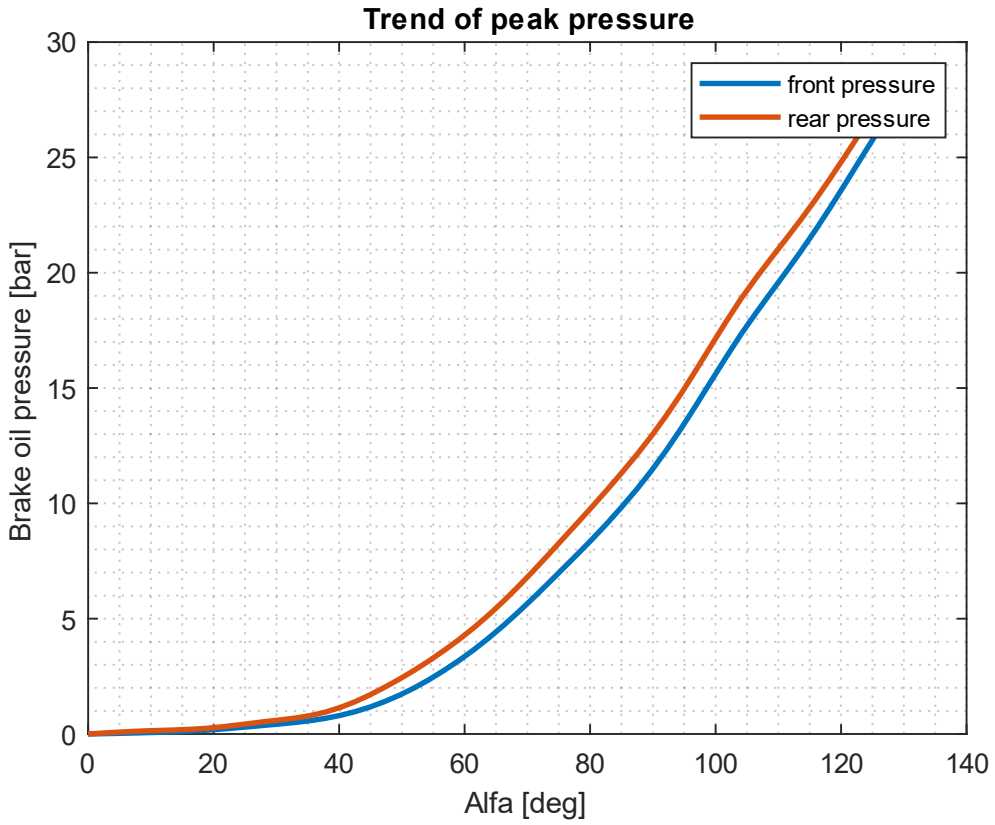

Figure 43 Trend of the peak pressure

This first plot has been evaluated interpolating the punctual values registered at the peak of the spike for each step. After a first sector in which the two pressures have a parabolic trend, it is visible an almost linear behaviour. During the linear phase the two signals proceed parallel.

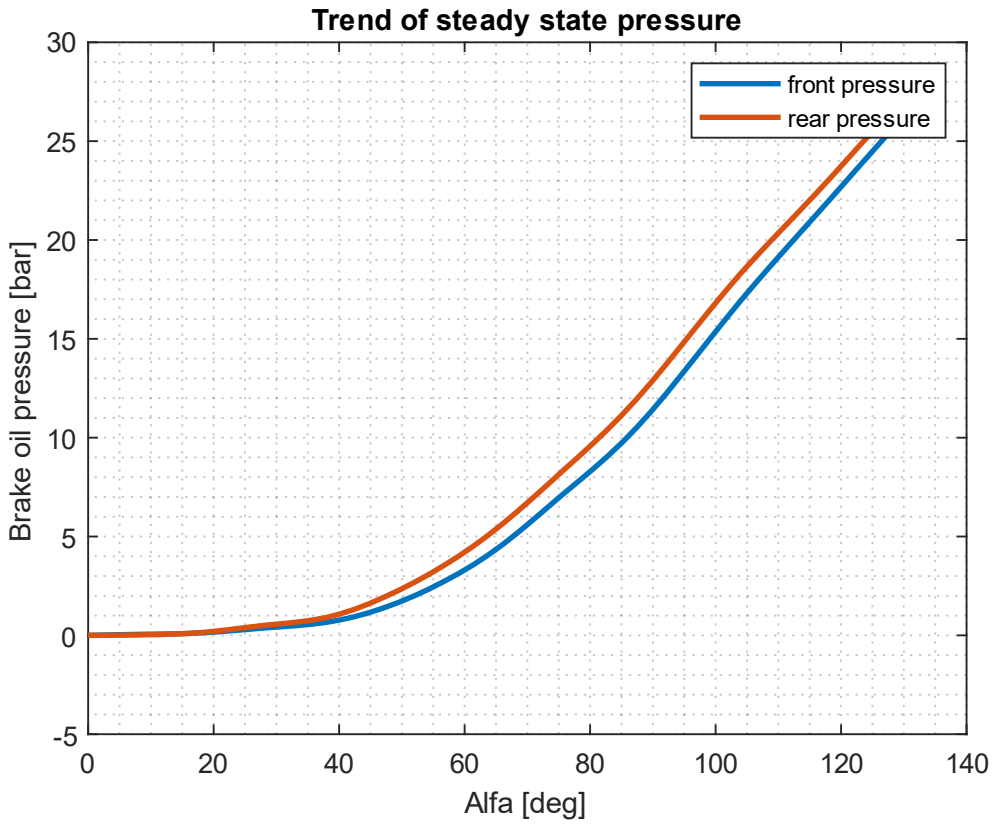

Figure 44 Trend of steady state pressure

The same observations can be done to the trend of the steady state pressure, measured at each iteration once the value was stable. Due to the parallelism between the signals the gap remains constant even if the pressure increase showing a slightly different behaviour compared to the one obtained in the multibody model (Figure 21). In the modelled system the two pressure trends inside the two lines have a slightly divergent behaviour increasing their difference according to the servomotor rotation. This difference can be imputated to the difference between the real braking line and the equivalent stiffness modelled in the multibody. The system modeled in this way takes into account that the behaviour remains constant during the movement of the master cylinder. This is not true in the real system because once the brake pads touch the brake discs, the equivalent stiffness increases. This limits the master cylinder movements and also the rotation of the balance bar. Due to this reason a possible future upgrade for this model could be to consider springs with bilinear behaviour that in the first section are softer and when the brake pads touch the brake discs begin more stiff. Anyway, even if the trends are parallel and not divergent, both the trends are linear exactly as in the model and with almost the same slope.

Controlled System

In this section an overlook about the controlled system performances will be done. Since the derivative term has been chosen null to reduce the oscillations in the transient phases, the controller is a PI with the aim to reduce the error between the actual pressure inside the front braking line and the desired one. If the controller is well designed the pressure should reach the desired pressure in a certain time and with a certain amount of transient phase. Let's consider a step reference test in which the request of pressure sudden increases up to a certain value. This test allows to understand the performances of the system and its controller.

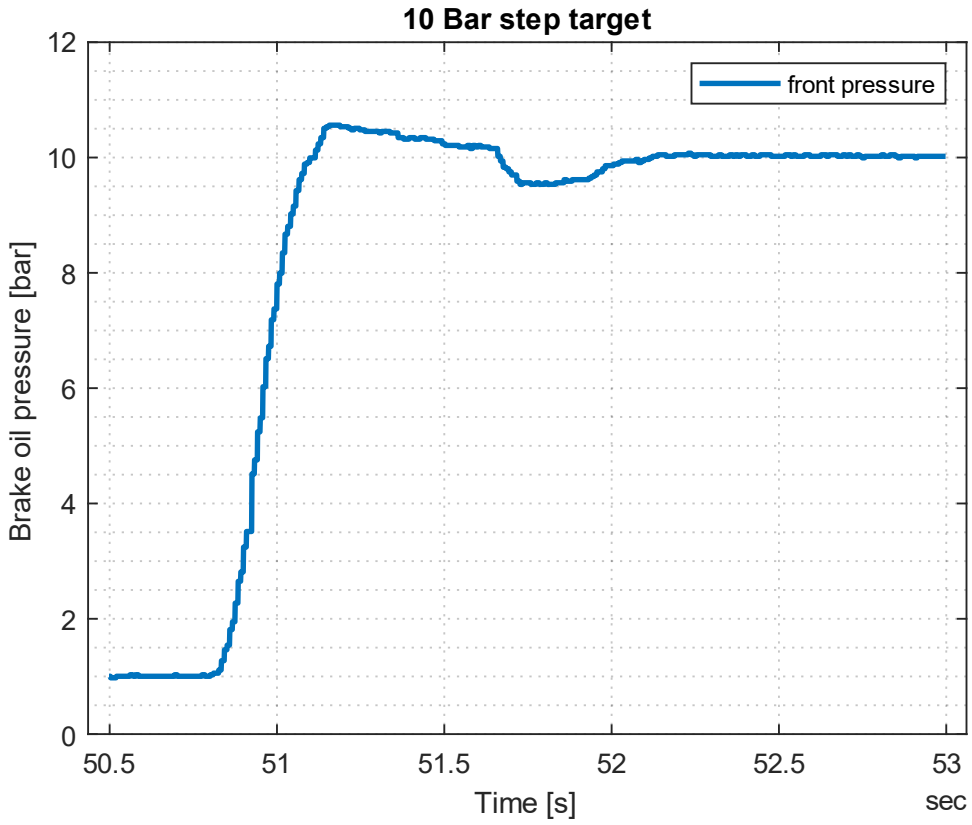

Figure 45 10 Bar step target

The step target imposed in this test is 10 bar. Looking at Figure 43 the trend of pressure follows a second order shape. Initially the pressure increases up to a peak higher than the target steady state value, then there is a valley in which the pressure is slightly lower and in the end the value of pressure is stable equal to the target one. The following characteristic factors can be evaluated:

- Rising time τ_R, that is the time needed for the system to achieve the 90% of the steady state value. In this case τ_R= 0.2 s, that is an acceptable value for this kind of application since it is almost equal to the average human reaction time [30].
- Settling time τ_S, that is the time needed to reach the steady state condition (considering anyway an error generally of 2% or 5%). In this case τ_S=1.36 s.
- Overshoot, that is the occurrence of the signal exceeding its target, and it is calculated with the equation:

$$\hat{s} = \frac{P_{max} - P_{\infty}}{P_{\infty}}$$

  In this case is $\hat{s}$ = 0.053.

Comparing the data collected in this test with the ones collected in Figure 40 is evident a certain difference of behaviour during the transient phase. Both the measurements show an initial peak value attributable to the sudden increase of the equivalent stiffness due to the contact of the brake pads against the brake discs. In the transient phase the test effectuated controlling only the motor position doesn't show an evident valley after the initial peak. In this condition the position control was only related to the internal logic measurement of the servomotor. In the test of figure 43 instead the closed loop control is done using the pressure as reference and the little valley before the steady state value could be related to the PI chosen parameter since after the peak exceeding the target the proportional term imposes a correction that makes the value lower than the reference. During the tests other configurations with less oscillations have been found but they used to have a slower dynamic response. This solution was the optimal one for our purposes.

Another test has been performed using as an input a random step target. This signal generates sudden changes in pressure request that are always embedded inside the ASB operating range. The idea of this test is to simulate a limit case scenario similar to a plausible track dynamic behaviour.

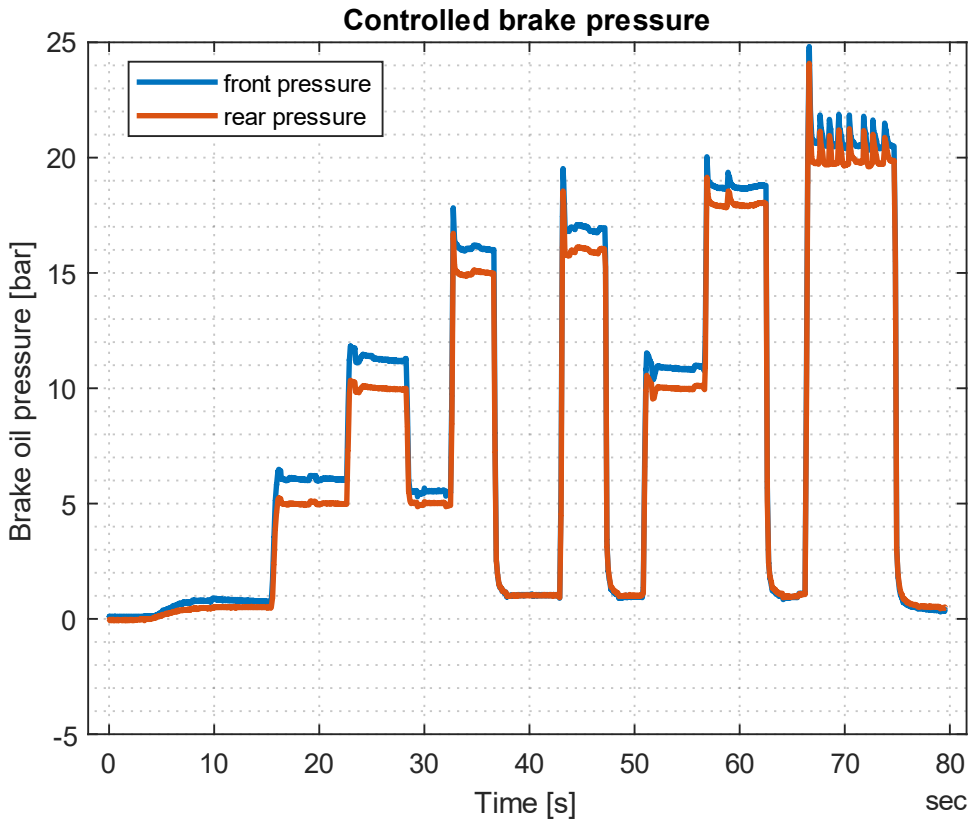

Figure 46 Random target controlled system

In the plot both the front and the rear pressure are reported even if the control loop is closed on the front brake line pressure sensor. During the test the ASB system performed multiple jumps of pressure always in about 0.2 seconds that is a relative short time for this application. From the test is visible the action of the balance bar that and the proportion between the target and the signal overshoot. Higher is the pressure reached and higher is the overshoot and therefore, the settling time. Anyway, if the general behaviour is considered the tests demonstrated the reliability and the speed of this system: in each operating point the ASB is able to reach the target pressure within a rising time equal to 0.2 seconds and keep the desired pressure until another target is imposed. Similarly to the step response test highlighted before, the peak overshoot is always related principally to the sudden stiffness increase, and here is also better visible the transient valley phase that is accentuated for higher pressure jumps. Logically higher is the initial error and higher will be the oscillation before the steady state. In the last phase there are more oscillations that can be related to higher correction of the PI due to the high peak pressure. Anyway, even if the controller were pushed to its limit operating area, the system never showed a divergent behaviour.

Conclusions

The aim of this thesis was to design an autonomous actuator classified as Autonomous System Brake, able to decelerate the vehicle with certain performances demanded by the Formula Student Driverless Rulebook. The design started from mathematical relations done on a simplified bi-dimensional brake pedal model. Here the layout of the system has been decided. Then, in order to develop the control logic, a three-dimensional parametrized multibody model that represent the whole system in its most significant components has been computed. From that model, some look up tables that link the PWM to the pressure inside the braking lines have been extracted and with a close loop controller they brought to a reliable and fast control both on the simulated and on the real vehicle. The validation of the multibody system shown some analogies but also some significant differences between the real system and the multibody one. In general, the behaviour is the same since in both systems the trend of pressure linearly depends on the servomotor position with almost the same slope, anyway the characteristic constant that describe the behaviour of the brake could be improved. An upgrade that could be done in the future to improve the simulation consistency is regarding the equivalent stiffness approach. In the approximation done in Chapter 1 - Preliminary Dimensioning, a simple equivalent spring has been considered. Anyway, looking at the results obtained by the tests, the behaviour of the system could be better represented by bilinear springs. Those could be less stiff in the first section in which the brake pads are not in contact with the brake discs yet, and then have a stiffer behaviour. The multibody system has been totally parametrized. Thanks to this choice, if any modification will be done on the real vehicle, the multibody model could be simply run with the new geometries (i.e. pulley diameter, position of the servomotor, geometries of the brake pedal, ect.) to obtain new lookup tables ready to control the new system. Some future upgrades for a further development of this autonomous system brake could be:

- Realize a pre-tensioning system for the metal cable to avoid the first nonlinear section.
- Better align the multibody model and the real system to have an exactly digital twin of the real system.
- Use a hardware in the loop (HIL) approach to build a test bench on which any test can be performed. This could improve the development phase.

- Perform more test on track to further improve braking effort and optimize the tire friction.

These upgrades could be done in the future with test done on the prototype in laboratory and on the track. The aim of this thesis was to design and build a functional electromechanical autonomous braking actuator. The ASB has been designed and produced and each target imposed at the beginning has been reached, obtaining also good results during races, both in static and dynamic events.

References

[1] How many cars are there in the world? Website: https://www.carsguide.com.au/car-advice/how-many-cars-are-there-in-the-world-70629

[2] How many cars there are in the world in 2022? Website: https://hedgescompany.com/blog/2021/06/how-many-cars-are-there-in-the-world/

[3] Taxonomy and Definitions for Terms Related to Driving Automation Systems for On-Road Motor Vehicles, Web link: J3016_202104https://www.sae.org/standards/content/j3016_202104/

[4] Pigeon, C., Alauzet, A., & Paire-Ficout, L. (2021). Factors of acceptability, acceptance and usage for non-rail autonomous public transport vehicles: A systematic literature review. Transportation research part F: traffic psychology and behaviour, 81, 251-270.

[5] Indy Autonomous Challenge. Website: https://www.indyautonomouschallenge.com/

[6] Ritchie, O. T., Watson, D. G., Griffiths, N., Misyak, J., Chater, N., Xu, Z., & Mouzakitis, A. (2019). How should autonomous vehicles overtake other drivers?. Transportation research part F: traffic psychology and behaviour, 66, 406-418.

[7] GPR, About Formula Student. Website: https://www.global-formula-racing.com/en/formula-student

[8] Formula Student Rules 2022, Website: https://www.formulastudent.de/fileadmin/user_upload/all/2022/rules/FS-Rules_2022_v1.0.pdf

[9] Consystem, Tecnologia LiDAR: che cosa è? come funziona? website: https://consystem.it/faq/tecnologia-lidar-che-cosa-e-come-funziona/

[10] E-con Systems, What is a stereo vision camera? Website: https://www.e-consystems.com/blog/camera/technology/what-is-a-stereo-vision-camera-2/

[11] Leidecker, H., Panashchenko, L., & Brusse, J. (2011, September). Electrical failure of an accelerator pedal position sensor caused by a tin whisker and discussion of investigative techniques used for whisker detection. In Proc. 5th International Symposium on Tin Whisker, Maryland (Vol. 14).

[12] Raffaele Manca:
Performance Assessment of an Electric Power Steering System for Driverless Formula Student Vehicles

[13] Gennaro Sorrentino (2020):
Design of autonomous control systems for a Driverless race car: Remote Emergency System and Autonomous State Machine

[14] Jain, P., & Garani, H. (2016). Analysis and Assessment of Dual Brake Circuits. International Journal of Mechanical Engineering and Technology, 7(5).

[15] Science Direct, Vehicle Handling Performance,
website: https://www.sciencedirect.com/topics/engineering/understeer

[16] Bhonge, A., Gunai, P., & Joshi, K. (2016). Design and Analysis of Brake and Gas Pedal. International Journal of Advanced Engineering Research and Science, 3(11), 236912.

[17] Ahmad, F., Mazlan, S. A., Zamzuri, H., Jamaluddin, H., Hudha, K., & Short, M. (2014). MODELLING AND VALIDATION OF THE VEHICLE LONGITUDINAL MODEL. International Journal of Automotive & Mechanical Engineering, 10.

[18] Kudarauskas, N. (2007). Analysis of emergency braking of a vehicle. Transport, 22(3), 154-159.

[19] Autoevolution. What is Brake By Wire and How It Works. Website: https://www.autoevolution.com/news/what-is-brake-by-wire-and-how-it-works-150856.html

[20] Sinha, P. (2011). Architectural design and reliability analysis of a fail-operational brake-by-wire system from ISO 26262 perspectives. Reliability Engineering & System Safety, 96(10), 1349-1359.

[21] Wikipedia, Linear actuator, Website: https://en.wikipedia.org/wiki/Linear_actuator

[22] Karanja, B., & Broukhiyan, P. (2017). Commercial vehicle air consumption: Simulation, validation and recommendation.

[23] Angadi, S. V., & Jackson, R. L. (2022). A critical review on the solenoid valve reliability, performance and remaining useful life including its industrial applications. Engineering Failure Analysis, 106231.

[24] HS-1005SGT Servo Specification, website: https://hitecrcd.com/products/servos/giant-servos/digital-giant-servos/hs-1005sgt-industrial-grade-giant-scale-servo/product

[25] Wikipedia, Multibody System, website: https://en.wikipedia.org/wiki/Multibody_system

[26] MathWorks Documentation, Multibody Modelling, website: https://it.mathworks.com/help/sm/multibody-modeling.html

[27] Wikipedia, Lookup Table, website: https://en.wikipedia.org/wiki/Lookup_table

[28] Arduino e i Servomotori, Roberto Beligni, website: https://www.makerslab.it/arduino-ed-i-servomotori/

[29] Bennett, S. (2001). The past of PID controllers. Annual Reviews in Control, 25, 43-53.

[30] Reference, What is the average human reaction time? Website: https://www.reference.com/world-view/average-human-reaction-time-64cbed7617fa4bd2